

intestazione repository dell'ateneo

Novel Curcumin loaded nanoparticles engineered for Blood-Brain Barrier crossing and able to disrupt Abeta aggregates

This is the peer reviewed version of the following article:

*Original*

Novel Curcumin loaded nanoparticles engineered for Blood-Brain Barrier crossing and able to disrupt Abeta aggregates / Barbara, Ruozi; Belletti, Daniela; Pederzoli, Francesca; Masoni, Martina; Keller, Johannes; Ballestrazzi, Antonio; Vandelli, Maria Angela; Tosi, Giovanni; Grabrucker, Andreas M.. - In: INTERNATIONAL JOURNAL OF PHARMACEUTICS. - ISSN 0378-5173. - 526:1-2(2017), pp. 413-424.

*Availability:*

This version is available at: 11380/1142358.1 since: 2017-07-12T15:31:14Z

*Publisher:*

*Published*

DOI:10.1016/j.ijpharm.2017.05.015

*Terms of use:*

openAccess

Testo definito dall'ateneo relativo alle clausole di concessione d'uso

*Publisher copyright*

(Article begins on next page)

Elsevier Editorial System(tm) for  
International Journal of Pharmaceutics  
Manuscript Draft

Manuscript Number: IJP-D-17-00411R1

Title: Novel Curcumin loaded nanoparticles engineered for Blood-Brain Barrier crossing and able to disrupt Abeta aggregates.

Article Type: Research Paper

Section/Category: Pharmaceutical Nanotechnology

Keywords: synapse, amyloid, Alzheimer's disease, BBB targeting nanoparticles, nanotechnology, curcumin

Corresponding Author: Professor Giovanni Tosi, PhD

Corresponding Author's Institution: University of Modena and Reggio Emilia

First Author: Barbara Ruozi, Associate Professor

Order of Authors: Barbara Ruozi, Associate Professor; Daniela Belletti, PhD; Francesca Pederzoli, PhD; Martina Masoni, Pharm.D.; Johannes Keller, MD; Antonio Ballestrazzi, PhD; Maria Angela Vandelli, Full Professor; Giovanni Tosi, PhD; Andreas M Grabrucker, Associate Professor

Abstract: The formation of extracellular aggregates built up by deposits of  $\beta$ -amyloid ( $A\beta$ ) is a hallmark of Alzheimer's disease (AD). Curcumin has been reported to display anti-amyloidogenic activity, not only by inhibiting the formation of new  $A\beta$  aggregates, but also by disaggregating existing ones. However, the uptake of Curcumin into the brain is severely restricted by its low ability to cross the blood-brain barrier (BBB). Therefore, novel strategies for a targeted delivery of Curcumin into the brain are highly desired. Here, we encapsulated Curcumin as active ingredient in PLGA (polylactide-co-glycolic-acid) nanoparticles (NPs), modified with g7 ligand for BBB crossing. We performed in depth analyses of possible toxicity of these NPs, uptake, and, foremost, their ability to influence  $A\beta$  pathology in vitro using primary hippocampal cell cultures. Our results show no apparent toxicity of the formulated NPs, but a significant decrease of  $A\beta$  aggregates in response to Curcumin loaded NPs. We thus conclude that brain delivery of Curcumin using BBB crossing NPs is a promising future approach in the treatment of AD.



Università degli Studi di Modena e Reggio Emilia  
**DIPARTIMENTO DI SCIENZE DELLA VITA**

Modena, April 26<sup>th</sup> 2017

Dear Editor,

Please find enclosed the revision version of our paper now entitled “**Novel Curcumin loaded nanoparticles engineered for Blood-Brain Barrier crossing and able to disrupt Abeta aggregates**”

We thank the referee and the editor, since we do think that after revision and following the suggestion of the referees, now the paper is increased in value and we hope to be now suitable for publication.

Attached and below, the list of changes

I thank you very much for your attention and please receive my warmest regards,

Giovanni Tosi  
Associate Professor  
Department of Life Sciences  
University of Modena and Reggio Emilia  
Italy

## IJP AUTHOR CHECKLIST

Dear Author,

It frequently happens that on receipt of an article for publication, we find that certain elements of the manuscript, or related information, is missing. This is regrettable of course since it means there will be a delay in processing the article while we obtain the missing details.

In order to avoid such delays in the publication of your article, if accepted, could you please run through the list of items below and make sure you have completed the items.

### Overall Manuscript Details

- Is this the final revised version? X
- Are all text pages present? X
- Are the corresponding author's postal address, telephone and fax numbers complete on the manuscript? X
- **Have you provided the corresponding author's e-mail address?** X
- **Manuscript type – please check one of the following:**
  - Full-length article X
  - Review article
  - Rapid Communication
  - Note
  - Letter to the Editor
  - Other
- **Manuscript section – paper to be published in:**
  - Pharmaceutical Nanotechnology section X
  - Personalised Medicine section

### Manuscript elements

- Short summary/abstract enclosed? X
- 3-6 Keywords enclosed? X
- Complete reference list enclosed? X
- Is the reference list in the correct journal style? X
- Are all references cited in the text present in the reference list? X
- Are all **original** figures cited in the text enclosed? X
  - Electronic artwork format? -----
- Are figure legends supplied? X
- Are all figures numbered and orientation provided? X
- Are any figures to be printed in colour? 
  - If yes, please list which figures here:-----
- If applicable, are you prepared to pay for reproduction in colour?
- Are all tables cited in the text supplied? X

### General

- Can you accept pdf proofs sent via e-mail? X

Reviewer #1: Barbara and co-workers report a study on the encapsulation of curcumin in polymeric nanoparticles modified with a glycopeptide. They propose this formulation as an approach to target CUR to the CNS. The study comprises the physicochemical characterization and *in vitro* studies on toxicity and effects on amyloid beta aggregates. However, in our opinion the manuscript needs a revision regarding some aspects, as detailed below:

1) Please, improve the introduction, taking into account previous studies with nanospheres and nanocapsules containing curcumin proposed for treatment of AD.

We improved as suggested by the reviewer.

2) Novelty of the study is not clear in the introduction and objective.

Notwithstanding the encapsulation of curcumin into nanoparticles is a well-known aspect, in this study we evaluated the possibility to stabilize therapeutic amounts of drug into engineered nanoparticles specifically designed to cross the BBB. We applied our own validated methodology by formulating g7-NPs using pre-formulation approach. Here, as a first step for the future application of the new loaded nanoparticles, we reported a technological characterization of the systems, but most of all the demonstration of the absence of toxicity and ability to reduce the aggregation of  $\beta$ -amyloid *in vitro*. We therefore improved the introduction by focusing on the objective of the study.

3) Was the amount of cryoprotectant not considered in the calculation of the yield? Why?

Trehalose was added to the formulation as cryoprotectant. More in detail, we added Trehalose at the end of the formulation and purification processes and immediately before the freeze dry process with the aim to protect nanoparticles from aggregation and possible deconstruction. Based on this technological process, the yield of formulation was calculated considering only the component used during the formulation process (PLGA and Cur), thus excluding both surfactant and trehalose. We corrected the formula in the text as suggested by the reviewer.

4) Do the particle size values represent the behavior before or after the freeze-drying process? How were the samples diluted after the drying process? Comparison between the particle size properties before and after the freeze-drying process is missing.

Data reported refers to value obtained before the freeze-drying process. We thanks the reviewer for the comment, and, for a more complete characterization, we added a complete table with data obtained after suspension of the freeze-drying NPs powder in distilled water.

We improve both Fig.1 legend and method section, for a complete description of samples.

5) Could the loading capacity and encapsulation efficiency be affected by the presence of CUR crystals (including nanocrystals) in the Freeze-dried powder? In other words, as CUR has a very low aqueous solubility, could it precipitate during the formulation? How can the authors refute the hypothesis of simultaneous presence of CUR crystals and nanoencapsulated CUR in the powders?

As reported by the reviewer, the low water solubility of curcumin could induce a precipitation of the not encapsulated drug during the formulation. In our protocol, the presence of surfactant (PVA at 1% v/v) assures that the part of drug, which remains outside from the nanoparticles, to stay complexed with PVA and perfectly in solution. Based on this observation, we did not observe any precipitate (yellow powder related to crystals of curcumin which should rapidly precipitate) during the formulation or during the washing process. PCS data of the formulation in the post purification step or in the post freeze-drying step in fact described the presence of monomodal population excluding the presence of crystals.

6) Were the sink conditions considered during the in vitro drug release analysis? Could the sustained phase of the release profile be explained by any saturation of the release medium? How much the delivery of CUR from the NPs (Fig. 1D) is different from the release from a bulk suspension?

The release study was carried out considering the sink conditions. Curcumin has a very low water solubility (1-10 µg/mL, *Jagannathan, R., et al., 2012. Temperature-dependent Spectroscopic evidences of curcumin in aqueous medium: a mechanistic study of its solubility and stability. J. Phys. Chem. B 116: 14533–14540*), thus reaching the sink condition in buffer resulted very difficult, thus requiring a large volume of water phase.

In this study, we chose to incubate loaded NPs in a medium composed by PBS and FBS (50%v/v), in order to mimic the physiological conditions. In this case, the presence of large amounts of proteins both produces a condition similar in vivo one and acts as a “carrier” for curcumin, released from nanoparticles thus increasing Curcumin solubility in the release medium and insuring sink conditions. Based on this fact, the conditions used in this study match the sink condition for the study of the release.

In absence of a dialyses bag or any other physical device commonly used to study the release of a drug from a nanoparticles, we decided not to evaluate the diffusion of Curcumin from bulk.

In this case, nanoparticles are not also a delivery system, but a strategy to improve solubility of the drug that on the contrary, without encapsulation, rapidly precipitates in water at the concentrations used in this study, thus quickly being not administrable. Based on this evidences, we think that the release of Cur from the nanopartilces should be considered as an objective data, not comparable with the release from the bulk.

7) Comparison between the encapsulated CUR and its non-encapsulated form is missing in the discussion and conclusion. What are the conclusions about the advantages of CUR encapsulation? The improved aqueous solubility and stability have been widely described for nanoencapsulated drugs and substances and it is not a novelty. Conclusion should be improved to highlight the novel contribution of the paper to the area. How can you conclude about the superior performance of the encapsulated CUR compared with CUR?

We improved the discussion conclusion section by following the suggestions of the reviewer.

8) Check for typos (proprieties, page 16).

Thanks, we checked the typos and corrected

Reviewer #2: This manuscript from Barbara et al. entitled "Targeted disruption of Amyloid beta aggregates by novel Curcumin loaded Nanoparticles International Journal of Pharmaceutics" describes the use of curcumin loaded particles to impede the formation of amyloid deposits. The authors use previously developed PLGA nanoparticles conjugated with a peptide supposed to target the blood brain barrier and

facilitate the translocation into the brain. The different tests presented tend to demonstrate that the particles have a significant effect in decreasing amyloid production in vitro and present low cellular toxicity at different cellular levels.

Overall, the manuscript is well presented with a lot of relevant experimental data. The approach used by the authors has been reported extensively but the study provides an interesting comprehensive view of the subtle mechanisms involved in curcumin therapeutical efficacy.

My main concerns are related to the characterization of the particles. The tests used to confirm the presence of the peptide at the surface of the particle is absolutely inconclusive. The authors should have performed a high resolution scan or even better, an NMR of the particles.

The presence of g7 onto the surface of nanoparticles was extensively demonstrated in previous studies. As previously reported, the use of a preformulative approach (in which g7 was conjugated to PLGA before the nanoparticles formulation) assure the g7, which is the hydrophilic moiety of the conjugated polymer, to be exposed on the surface, at the interface with water. In this way, the exposed peptide was able to mediate the BBB passage of PLGA NPs as demonstrated by pharmacological evidences (*Tosi G, et al., 2011. Investigation on mechanisms of glycopeptide nanoparticles for drug delivery across the blood-brain barrier. Nanomedicine 6:423-36., Salvalaio M, et al., 2016. Targeted Polymeric Nanoparticles for Brain Delivery of High Molecular Weight Molecules in Lysosomal Storage Disorders. PLoS One. 11:e0156452. Valenza M, et al., 2015. Cholesterol-loaded nanoparticles ameliorate synaptic and cognitive function in Huntington's disease mice. EMBO Mol Med. 7:1547-64. Tosi G, et al., 2007. Targeting the central nervous system: in vivo experiments with peptide-derivatized nanoparticles loaded with Loperamide and Rhodamine-123. J Control Release. 122:1-9).*

As ESCA is one of the most versatile tools in identifying the chemical species on a surface, we used this protocol for surface characterization in order to confirm the g7 exposure on the surface of Curcumin loaded nanoparticles.

ESCA is a surface analysis technique that provides elemental and binding energy information about a material's surfaces and interfaces. Characterized by an average depth of measurement of approximately 5 nm. (*Vickerman, J.C., et al., The Principal Techniques, 2nd Edition. Chapter 3. Electron Spectroscopy for Chemical Analysis*)

In this study, we reported ESCA characterization of unloaded and unmodified (NPs), unloaded and modified (g7-NPs) and loaded and modified nanoparticles (g7-NPs-Cur). Both sample were analyzed as dehydrated nanoparticles on an inert support. All the operations for sample preparation were carried out in a laminar flow hood to prevent any kind of contamination. Based on the assumed that all components of nanoparticles (PLGA, PVA and curcumin) are composed of C, H and O the signal typical of N should be related to the peptide exposed on the surface. As reported in results section, N signal was clearly detected in both g7-NPs and g7-NPs-Cur.

The presence of N signal assure that i) g7 is exposed on surface; ii) unless curcumin is partially exposed on the surface it not completely covered the peptide on nanoparticles surface.

We implemented the section "formulation and characterization of novel nanoparticles".

100% of release in less than 5 h seems really fast for nanoparticulate system. Did the author checked if they rather had micelles instead of particles?

As reported in Figure 1, 100% of release in reached in 3000 min which correspond to 50 hours and is more concordant with a nanoparticles release.

Curcumin is well known to degrade very fast at pH 7.4. The authors should explain how they could obtain 100 % of release without any loss.

As reported by the reviewer, curcumin rapidly decomposed at 37°C and pH 7.4. However, it is known that the stability of curcumin is significantly increased in serum added medium as in blood. Several studies recently confirmed the high affinity nature of curcumin binding to BSA [ *Borsari, M., et al. 2002. Inorg. Chem. Acta., 328, 61; Barik, K. I. et al., 2003. Photochem. Photobiol., 77, 597*]. The interaction with BSA has a double effect of solubilizing a higher number of molecules and simultaneously the unique ability in offering a strong protection from the oxidative and UV irradiation damage. By this way, the condition selected for the study (PBS/FBS 50/50 v/v) assured Curcumin to keep stable in the release medium.

The internalisation test using quantum dots is not described anywhere in the manuscript. Since it is a very important control experiment to validate the authors hypothesis, I would strongly recommend the authors to provide more conclusive data.

As suggested by the reviewer, we insert the internalization study into the text.

Some minor points:

-the title is not appropriate since no targeting capability was tested in the manuscript

We agree with the referee and change the title in:

-Novel Curcumin loaded nanoparticles engineered for Blood-Brain Barrier crossing and able to disrupt Abeta aggregates.

-some graphics are not referenced in the the text.

For example:Figure 1E, Table S1 and Fig S1 are not referenced anywhere in the text, so what am I suppose to understand with these data.

We inserted referenced figures along the text

-Some figure legends contain huge amount of information that should be included in the method section

We re-write figure legends deleting or shifting information. More in detail, we deleted some parts describing results and statistical analyses where it described not-significant data. Some significant data were shifted in the text.

Comments from the editor:

1. Please make sure that the resolution of all figures, including the graphical abstract, is sufficiently high, and that all text and numbers are clearly visible.

done

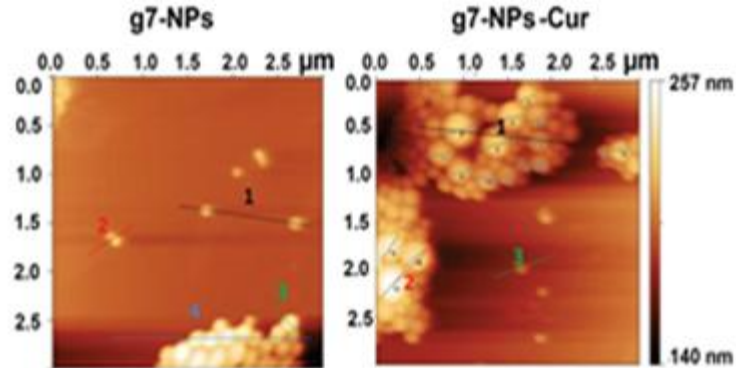
2. As requested by reviewer #2, please shorten the figure legends.

done

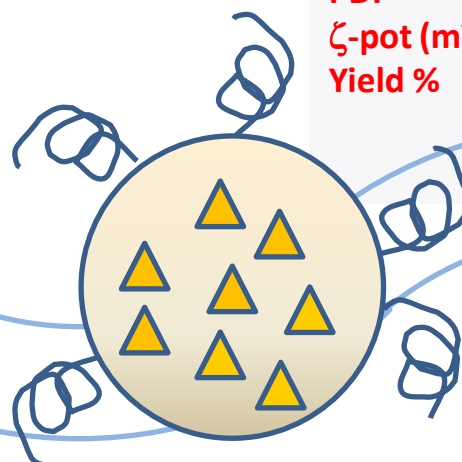


For further assistance, please visit our customer support site at <http://help.elsevier.com/app/answers/list/p/7923>. Here you can search for solutions on a range of topics, find answers to frequently asked questions and learn more about EES via interactive tutorials. You will also find our 24/7 support contact details should you need any further assistance from one of our customer support representatives.

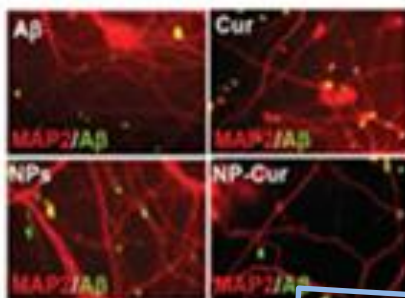
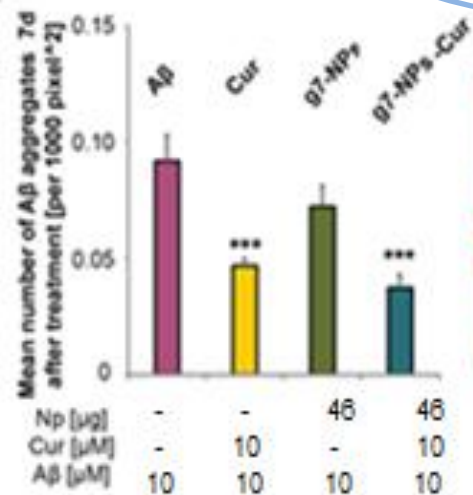
## Chemico-physical characterization






<b>Z-Aver. (nm)</b>	202(6)	204(10)
<b>PDI</b>	0.03(0.02)	0.07(0.02)
<b>ζ-pot (mV)</b>	-13(1)	-13(2)
<b>Yield %</b>	88(3)	97(2)
		<b>LC%</b> 3.1(0.8)
		<b>EE%</b> 60(6)



## In vitro studies (Alzheimer's disease)



-  g7 for BBB crossing
-  PLGA NPs
-  Curcumin

## **Novel Curcumin loaded nanoparticles engineered for Blood-Brain Barrier crossing and able to disrupt Abeta aggregates.**

Ruozi Barbara<sup>1</sup>, Daniela Belletti<sup>1</sup>, Francesca Pederzoli<sup>1</sup>, Martina Masoni<sup>1</sup>, Johannes Keller<sup>2</sup>, Antonio Ballestrazzi<sup>5</sup>, Maria Angela Vandelli<sup>1</sup>, Giovanni Tosi<sup>1#</sup>, Andreas M. Grabrucker<sup>2,3,4</sup>

<sup>1</sup>Department of Life Sciences, University of Modena and Reggio Emilia, Italy

<sup>2</sup>WG Molecular Analysis of Synaptopathies, Neurology Dept., Neurocenter of Ulm University, Ulm, Germany

<sup>3</sup>Institute for Anatomy and Cell Biology, Ulm University, Ulm, Germany

<sup>4</sup>Department of Biological Sciences, University of Limerick, V95PH61 Limerick, Ireland

<sup>5</sup>Department of Physical Sciences, Informatics and Mathematics, University of Modena and Reggio Emilia, Italy

#Corresponding author

Prof. Dr. Giovanni Tosi

Department of Life Sciences, University of Modena and Reggio Emilia

Modena, Via Campi 103, Italy

Tel.: +39 059 2058563

Email: giovanni.tosi@unimore.it

Running title: “*Targeting ABeta by curcumin NPs*”.

Keywords: synapse, amyloid, Alzheimer’s disease, BBB targeting nanoparticles, nanotechnology, curcumin

## **Abstract**

The formation of extracellular aggregates built up by deposits of  $\beta$ -amyloid ( $A\beta$ ) is a hallmark of Alzheimer's disease (AD). Curcumin has been reported to display anti-amyloidogenic activity, not only by inhibiting the formation of new  $A\beta$  aggregates, but also by disaggregating existing ones. However, the uptake of Curcumin into the brain is severely restricted by its low ability to cross the blood-brain barrier (BBB). Therefore, novel strategies for a targeted delivery of Curcumin into the brain are highly desired. Here, we encapsulated Curcumin as active ingredient in PLGA (polylactide-co-glycolic-acid) nanoparticles (NPs), modified with g7 ligand for BBB crossing. We performed in depth analyses of possible toxicity of these NPs, uptake, and, foremost, their ability to influence  $A\beta$  pathology *in vitro* using primary hippocampal cell cultures. Our results show no apparent toxicity of the formulated NPs, but a significant decrease of  $A\beta$  aggregates in response to Curcumin loaded NPs. We thus conclude that brain delivery of Curcumin using BBB crossing NPs is a promising future approach in the treatment of AD.

## Introduction

Alzheimer's disease (AD) is the most common cause of dementia among an estimated prevalence of 46.8 million people worldwide suffering from some form of dementia in 2015 ([www.alz.co.uk/research/world-report-2016](http://www.alz.co.uk/research/world-report-2016)). Clinically, AD shows strong anterograde amnesia and a reduction of semantic knowledge. Furthermore, changes in personality and temper were reported ([Butters et al., 1987](#)). AD is a multi-factorial neurodegenerative disorder pathologically characterized by deposits of  $\beta$ -amyloid ( $A\beta$ ) in senile plaques, intracellular neurofibrillary tangles (NFTs) comprised of hyper-phosphorylated aggregates of microtubule associated with tau protein, synaptic dysfunction, and neuronal death ([Schellenberg and Montine, 2012; Perl, 2010; Gallo et al., 2007](#)).

The amyloid precursor protein (APP) is a transmembrane polypeptide of 770 amino acids. In its physiological form, it is known for neurotrophic activity, while in AD, a pathological deposition of a 42 amino acid long cleavage product of APP,  $A\beta_{1-42}$  occurs. Under physiological conditions, APP is processed into non-aggregating peptides by  $\alpha$ -secretases. Genetic predisposition and/or environmental factors lead to differential processing of APP by  $\beta$ - and  $\gamma$ -secretases in AD ([Vassar et al., 1999](#)), which results in the formation of mainly extracellular  $A\beta$  aggregates. The  $A\beta$  monomers form dimers, oligomers, protofibrils and mature fibrils.  $A\beta$  modifications like phosphorylation have been shown to increase aggregation and toxicity ([Kumar and Walter, 2011](#)).

Amyloid plaques are big and inhomogeneous aggregates of  $A\beta$ , other peptides, and also AGE's (Advanced Glycation endproducts), which are built by non-enzymatic glycosylation. The plaques cause microglial activation and neuroinflammation. In addition or as result, synaptic loss is well described and has been attributed to a combination of toxic effects such as, among others, increased oxidative stress, synaptic  $A\beta$  toxicity, and/or zinc sequestration

by A $\beta$ . Synaptic loss as well as a decrease in overall cell number both correlate strongly with cognitive impairment in AD ([Butterfield, 1997](#)).

The diarylheptanoid Curcumin (Cur) is the main Curcuminoid found in the rhizome of the Turmeric/*Curcuma longa* plant. The root contains about 3-5 % Curcuminoids of which between 50-60 % are Cur with its main conformation (1,7-Bis-(4-hydroxy-3-methoxyphenyl)-hepta-1,6-dien-3,5-dion). A variety of physiological effects have been described for Cur in the last years. For example, Cur was reported to act as antioxidant due to its ability to neutralize radicals by two phenolic groups. Further, Cur has been shown to activate Nrf2 (Nuclear factor 2) resulting in the increased expression of the antioxidant responsive element (ARE) ([Esatbeyoglu et al., 2012](#)). In addition, Cur has been shown to act anti-inflammatory by modulation of Nf $\kappa$ B (Nuclear factor  $\kappa$ B) signaling ([Lin et al., 1997](#)). Most importantly, Cur was reported to possess anti-amyloidogenic properties. Cur can not only inhibit the formation of new A $\beta$  aggregates but also disaggregate existing ones ([Yang et al., 2005](#)). Additionally, increased neuronal cell viability and neurite formation was reported ([Ray and Lahiri, 2009](#)).

Unfortunately, Cur displays a low bioavailability and solubility. To overcome these limitations, which strongly hamper the applicability in clinical use of Cur, different drug delivery systems were investigated as strategies to stabilize the active, to reduce its metabolism and to prolong its circulation within the body, thus achieving more bioavailable formulations of Cur. In fact, Cur was encapsulated in liposomes, solid lipid microparticles, or nanoparticles using both natural (i.e chitosan) or synthetic polymers (polylactide-co-glycolide: PLGA, poly(n-butyl cyanoacrylate): PBCA). These nanoformulations were developed for preclinical studies on cancer, inflammation, wound healing, and other pathological conditions, which demonstrated enhanced therapeutic efficacies, when

nanoformulation strategies were applied in comparison with free Cur (*Lazar et al., 2013; Subramani et al., 2017, Hussain et al., 2017*).

The properties of Cur against inflammation and oxidative stresses were also investigated with references to brain diseases, in which these events represent both a pathological hallmark and possible causes of the progression of the diseases. Above physico-chemical “negative” properties of Cur, another major issue, considering the application in brain diseases, consists of the poor penetration of Cur across the Blood-Brain Barrier (BBB) (*Anand et al., 2007*).

The BBB describes the physiological barrier between the blood circulatory system and the central nervous system (CNS). The physiological function of the BBB is of major importance for maintaining a normal brain environment enabling the tight regulation of ion hemostasis and also protecting the CNS from circulating pathogens or toxins (*Abbott et al., 2010*). The development of new strategies to enhance Cur brain delivery based on colloidal carriers is of great importance, since **engineered** nanocarriers can protect drugs and deliver them across the BBB to target brain cells in a non-invasive way (*Tosi et al., 2008*). **To our knowledge, only few studies approached the formulation of Cur nanoparticles designed to target the brain. More in details nanoparticles functionalized with apolipoprotein E mimicking lipoprotein particles (*Mulik et al., 2010*) or surface engineered with Tat-1 peptide-derived from tetanus toxin (*Mathew et al., 2012*) were proposed as potential tools to transport Cur into the brain and tested *in vitro*.**

In our research paper, we proposed the application of a new technology for drug administration in the brain (*Vergoni et al., 2009; Tosi et al., 2010*), based on the formulation of biodegradable polymeric (PLGA) nanoparticles (NPs) loaded with Cur and modified with a glycopeptide (g7) able to cross the BBB (*Costantino et al., 2005; Tosi et al., 2007; Tosi et al., 2011*). Notably, both FDA and EMA approved PLGA in various drug delivery systems in humans (*Mundargi et al., 2008*), as confirmed by a number of marketed products (i.e.,

Lupron Depot, Nutropin Depot). Here, Cur loaded PLGA g7-NPs were tested for toxicity, targeted delivery, and biological activity using an *in vitro* model for AD, thus opening the pave for the future applications in *in vivo* animal model for evaluation of the efficacy in AD management.

## Materials and Methods

### Materials

Poly(D,L-lactide-co-glycolide) (PLGA, RG503H, MW near to 11,000) was used as received from the manufacturer (Boehringer-Ingelheim, Ingelheim am Rhein, Germany). Gly-L-Phe-D-Thr-Gly-L-Phe-L-Leu-L-Ser(O- $\beta$ -D-Glucose)-CONH<sub>2</sub> (g7) was prepared as described previously and conjugated with PLGA to obtain g7-PLGA ([Tosi et al., 2011](#); [Vergoni, et al., 2009](#); [Costantino et al., 2005](#); [Grabrucker et al., 2011a](#); [Tosi et al., 2013](#)). PLGA derivatization yields were confirmed by NMR, from the relative peak area of the signals at 7.2–7.5 ppm, corresponding to the aromatic protons of the Phe present and from the multiplet at 1.80–1.60 ppm, corresponding to the protons of the methyl groups of the polymer, respectively, and resulted to be in the range of 30–40  $\mu$ mol peptide/g of polymer.

Curcumin (Cur) was obtained by Sigma Chemical Co. (St. Louis Mo, USA). Polyvinyl alcohol (PVA), MW near to 15,000 Da was provided from Fluka (Milano, Italy). A Milli-Q water system (Millipore, Bedford, MA, USA), supplied with distilled water, provided high-purity water (18  $\Omega$ ) for NPs preparation. All the solvents were of analytical grade, and all other chemicals [ethyl(dimethylaminopropyl) carbodiimide (EDC), N-Hydroxysuccinimide (NHS), trehalose dihydrate (C<sub>12</sub>H<sub>22</sub>O<sub>11</sub>·2H<sub>2</sub>O), 2-(N-morpholino) ethanesulfonic acid (MES)] were obtained commercially and used without further purification.

Primary antibodies were purchased from Synaptic Systems (Bassoon), biorbyt (IkB), Sigma Aldrich (MAP2), Merck Millipore (OC), and Cell Signaling (PARP). Secondary Alexa Fluor



conjugated antibodies were purchased from Invitrogen. Secondary HRP conjugated antibodies were purchased from Dako. Synthetic A $\beta$  peptide, human A $\beta$ <sub>(1-42)</sub>, was purchased from American Peptides (Sunnyvale, CA, USA) and AnaSpec Inc. (San Jose, CA, USA). Unless otherwise indicated, all other chemicals were obtained from Sigma-Aldrich.

## **Methods**

### *Preparation of nanoparticles*

Cur loaded NPs (g7-NPs-Cur) were prepared by oil-in-water simple emulsion/solvent evaporation method as described in literature with some modifications in the preparation procedure ([Mainardes et al., 2005](#); [Bondioli et al., 2010](#)). Briefly, a mixture composed by g7-PLGA (9 mg), PLGA (91 mg) and Cur (5 mg, 5% w/w dry weight of polymer) were dissolved in 3 mL of dichloromethane. The polymer/drug organic solution was emulsified in 12 mL of 1% w/v aqueous solution of PVA under sonication (55 W for 60 sec) at 5°C. Then, the emulsion was mechanically stirred (1,500 rpm) for at least 3 h (RW20DZM, Janke&Kunkel, IKA-Labortechnik, Staufen, Germany) at r.t. until complete evaporation of the solvent. As control, empty (NPs) and empty functionalized nanoparticles (g7-NPs) were formulated applying the same technology.

### *Purification and collection of the NPs*

All NPs preparations were purified by an ultracentrifugation process carried out at 17,000 rpm for 10 min (4°C; Sorvall RC28S, Dupont, Brussels, Belgium) to remove the un-formed material and the free surfactant fraction. The NPs were washed three times with water, re-suspended in water (5 mL) and freeze-dried (-60°C, 1x10<sup>-3</sup> mm/Hg; LyoLab 3000, Heto-Holten) by using D-(+)-trehalose (Fluka–Sigma–Aldrich) as cryo-protectant (1:1 w/w polymer/trehalose ratio). The yield (Yield%) was calculate as follows:

$$\text{Yield (\%)} = S_{fd}/C_{tot} \times 100$$

$S_{fd}$  is the amount (mg) of freeze dried samples (excluded residual PVA and anhydrous trehalose) and  $C_{tot}$  is the total amount (mg) of polymer and Cur weighted for the preparation.

#### *Atomic force microscopy*

Atomic force microscopy (AFM) was used to clarify the morphology of the samples. The atomic force microscopical observations were performed with an Atomic Force Microscope (Park Instruments, Sunnyvale, CA, USA) at about 20°C operating in air and in Non-Contact (NC) mode using a commercial silicon tip-cantilever (high resolution noncontact “GOLDEN” Silicon Cantilevers NSG-11, NTMDT, tip diameter = 5–10 nm; Zelenograd, Moscow, Russia) with stiffness about 40 Nm<sup>-1</sup> and a resonance frequency around 170 kHz. After the purification, the samples were dispersed in distilled water and applied on a freshly cleaved mica disk (1 cm × 1 cm); 2 min after the deposition, the water excess was removed using blotting paper. The AFM images were obtained with a scan rate 1 Hz and processed using a program obtained from Gwyddion (Department of Nanometrology, Czech Metrology Institute, Brno, Czech Republic). Images were flattened using second-order fitting to remove [sample tilt] background curvature and slope from the images.

#### *Particle Size and Z-potential analysis*

The mean particle size (Z-average) and the polydispersity index (PDI) were determined at r.t. by photon correlation spectroscopy (PCS) using a Zetasizer Nano ZS (Malvern, UK; Laser 4 mW He–Ne, 633 nm, Laser attenuator Automatic, transmission 100–0.0003%, Detector Avalanche photodiode, Q.E. > 50% at 633 nm). The Z-potential ( $\zeta$ -pot) was measured using the same equipment with a combination of laser Doppler velocimetry and phase analysis light scattering (PALS). All the data are the means of the least three determinations carried out for

each preparation lot, referring to a suspension of NPs in distilled water before and after lyophilization.

#### *Determination of the amount of PVA residual*

As the residual PVA associated with the NPs could affect the physical properties and the cellular uptake, the amount of PVA was determined by a colorimetric method based on the formation of the colored complex between two adjacent hydroxyl groups of PVA and an iodine molecule ([Joshi et al., 1979](#)). Briefly, 5 mg of a freeze-dried sample were solubilized in 1 mL of DCM. Then, 2 mL of distilled water were added and the organic solvent was evaporated at r.t. under stirring (2 h). The suspension was filtered (cellulose nitrate filter, porosity 0.45  $\mu\text{m}$ , Sartorius, Firenze, Italy) to remove the polymeric residue and 1 mL of the aqueous solution was treated with 2 mL of 0.5 M NaOH for 15 min at 60°C. The solution was neutralized with 900  $\mu\text{L}$  of 1 N HCl and the volume adjusted to 5 mL with distilled water. Then, 3 mL of a 0.65 M solution of boric acid, 0.5 mL of a solution of  $\text{I}_2/\text{KI}$  (0.05 M/0.15 M), and 1.5 mL of distilled water were added. PVA concentration was determined measuring the absorbance at 690 nm after 15 min incubation at r.t. in comparison with a standard plot of PVA prepared under the same experimental conditions.

#### *Determination of drug loading capacity and encapsulation efficiency*

Cur loaded into g7-NPs-Cur was extracted and quantified by high performance liquid chromatography (HPLC). Briefly, an exact amount of NPs (about 1 mg) was solubilized into 0.5 mL of chloroform by using a bath sonicator for 5 min. Then, 4 mL of isopropyl alcohol were added to precipitate the polymer. The mixture was filtrated through PTFE filter (0.2  $\mu\text{m}$ , Sartorius, Firenze, Italia) and the solution analyzed by HPLC. The HPLC apparatus (JASCO Europe, Cremella, Italy) comprised a Model PU2089 pump provided with an

injection valve with a 50  $\mu\text{L}$  sample loop (Model 7725i, Jasco) and the UV/VIS detector (UV1575, Jasco). The analysis was performed in isocratic conditions, at a flow rate of 1 mL/min and at r.t. on a column HC-C18 (250mm x 4.60 mm, 5  $\mu\text{m}$ , Agilent Technologies) equipped with a security guard. The mobile phase was a mixture 41:23:36:1 (v/v/v/v) of acetonitrile, methanol, water and acetic acid. Chromatographic peak areas of the samples were recorded and analyzed using a JASCO software (JascoBorwin 1.5) and the concentration was calculated using the calibration curve previously set up (linearity was assumed in the range 0.3–9.5  $\mu\text{g/mL}$ ;  $r^2 = 0.9951$ ). The encapsulation ability of NPs was evaluated considering the encapsulation efficiency (EE%) and the loading capacity (LC%) calculated using the following equations:

$$\text{EE\%} = D / T_d \times 100$$

$$\text{LC\%} = D / W \times 100$$

where D is the amount of the encapsulated drug,  $T_d$  is the amount of drug added for the preparation and W is the weight of NPs (polymer + drug).

All the data are expressed as the mean of at least three determinations.

#### *In vitro release studies*

For each time point, an exact amount of g7-NPs-Cur (about 2 mg) was suspended in 1 mL of a 50% v/v of serum solution (FBS) at 37°C under electromagnetic stirring. After the incubation time (30 min, 3, 6, 24, 30, 48, 72 h), the suspensions were centrifuged (13,000 rpm for 15 minutes) to separate NPs (with possible adsorbed serum protein and residual loaded Cur) that precipitates from supernatant. The possible serum proteins adsorbed on NPs surface were quantified by colorimetric assay bicinchoninic acid (BCA) as described by manufacturer (Micro BCA protein assay kit composed of reagent A (alkaline tartrate-carbonate buffer), reagent B (bicinchoninic acid solution) and reagent C (copper sulfate solution), purchased from

Thermo Fisher Scientific Inc (Milan, Italy)) and subtracted from dried pellet to obtain the amount of NPs recovered after centrifugation. Residual Cur in NPs was extracted and quantified from pellet as described above.

### *Cell culture*

Primary hippocampal cultures were prepared from rat brains (embryonic day 18) as described before ([Grabrucker et al., 2009](#)). In brief, the brains were collected in pre-chilled Hank's balanced salts solution (HBSS, GE Healthcare Life Sciences, UK) and the hippocampi were dissected. Hippocampi in 1800  $\mu$ L HBSS were then trypsinized with 200  $\mu$ L Trypsin 2.5% (Invitrogen, USA) for 20 min at 37°C. After 5 washing steps, cells were re-suspended in 1600  $\mu$ L HBSS and 400  $\mu$ L DNase 1 (0.01%). The suspension was filtered through a 125  $\mu$ m sieve and incubated with 18 mL of DMEM (Dulbecco's Modified Eagle Medium, GIBCO, USA), 10% FCS, 1% glutamine and 1% penicillin-streptomycin. Cells were then counted in the Neuburger-Chamber. After preparation, the hippocampal neurons were seeded on poly-l-lysine (0.1 mg/mL; Sigma-Aldrich) glass coverslips in a 24 well plate at a density of 30,000 cells/well or 10 cm petri dish at a density of  $3 \times 10^6$  cells/dish. Cells were grown in Neurobasal<sup>TM</sup> medium (Life Technologies), complemented with B27 supplement (Life Technologies, USA), 0.5 mM L-Glutamine (Life Technologies) and 100 U/mL penicillin/streptomycin (Life Technologies) (resulting in NB+++ medium) and maintained at 37°C in 5% CO<sub>2</sub>. All animal experiments were performed in compliance with the guidelines for the welfare of experimental animals issued by the Federal Government of Germany and by the local ethics committee of Ulm University (ID Number: O.103).

### *Treatment of hippocampal cells*

A $\beta$ <sub>(1-42)</sub> peptides were initially dispersed in dH<sub>2</sub>O at a concentration of 1 mg/mL and thereafter stored at -20°C until use. Further dilutions of the peptides were performed in the

culture medium (NB+++). Pure Cur was diluted to 1 mM in DMSO and stored at -20°C. Further dilutions were performed in the culture medium (NB+++). To carry out the treatment with NPs, neurons were seeded in a total volume of 500 µl per well (24 well plate) or 10 mL per 10 cm petri dish in NB+++ medium. Freeze dried NPs samples were re-suspended in HBSS under sonication (Emmi-05P Sonicator, Emag, Germany) to have a starting batch for further dilution in culture medium (NB+++) to administer different concentration (10, 20, 40 µM final concentration) of Cur by NPs in cells. NP stock solutions were prepared according to the calculated Cur content and the volume of HBSS adjusted accordingly. Stock solutions of empty NPs were prepared to match the amount of NP per mL of Cur loaded NPs.

#### *Immunocytochemistry*

For immunofluorescence, the primary cultures were fixed with 4 % paraformaldehyde (PFA)/ 4% sucrose/PBS at 4°C for 20 min and processed for immunocytochemistry. After washing 3x5 min with 1x PBS containing 0.2% Triton X-100 at RT, blocking was performed with 10% FBS/ 1x PBS for 1 h at r.t. Subsequently, samples were incubated with primary antibody at r.t. for 2 h or at 4°C overnight. After a 3x5 min washing-step with 1x PBS, incubation with the secondary antibody coupled to Alexa488, Alexa568 or Alexa647 followed for 1 h. Cell nuclei were counterstained with DAPI and coverslips subsequently mounted using Vecta Mount (Vector Laboratories, USA).

#### *Determination of cell death (apoptosis versus necrosis)*

Toxicity of the samples after treatment was characterized by a healthy/apoptotic/necrotic cell detection kit (Promokine, Germany) using primary hippocampal rat cultures at DIV 14 on 24-well plates (in 500 µL medium per well), according to the manufacturer's protocol. In brief, cells were washed with 1x binding buffer and incubated for 15 min at r.t. protected from light

with a staining solution containing 100  $\mu$ L of 1x binding buffer, 5  $\mu$ L of FITC-Annexin V, 5  $\mu$ L of Ethidium Homodimer III and 5  $\mu$ L of Hoechst 33342. Cells were washed twice with 1x binding buffer. Then, the cells were fixed with (PFA)/PBS and 1.25 mM CaCl at r.t. for 15 min. Coverslips were mounted on slides with a drop of Vecta Mount. As positive control, apoptosis was induced with 500  $\mu$ L of 70% ethanol.

### *Protein Biochemistry*

Treated primary hippocampal rat cultures at DIV 14 were lysed and homogenized in lysis buffer (150 mM NaCl, 1% Triton® X-100, 50 mM Tris HCl, pH 8.0) containing protease inhibitor (Roche, Mannheim, Germany) at 4°C for 2-3 h by overhead shaking before being centrifuged for 15 min at 3,200 x g. **Experiments were performed in Petri dish.** The resulting supernatant was then used for analyses. Subcellular fractions were isolated as described previously with minor modifications (*Schmeisser et al., 2012*). To detect the fibrillation state and concentration of A $\beta$  in the supernatant, Ultra Centrifugal Filters from Amicon (Germany) were used to increase the sample concentration. 500  $\mu$ l of the supernatant were loaded into a filter and spun with 14,000 rpm for 10 min. The filter was then placed upside down in a new tube and spun again with 1,000 rpm for 10 min.

*Western blotting:* For western blot experiments, membrane-associated fractions from rat brains (P2) were used. Proteins were separated by SDS-PAGE and blotted onto Nitrocellulose membranes. Immunoreactivity was visualized using HRP-conjugated secondary antibodies and the SuperSignal detection system (Pierce, Upland, USA).

*Dot blotting:* For Dot blots experiments, a PVDF membrane was incubated with 100% methanol followed by water for few seconds and subsequently with Transfer Buffer + SDS for 3 min. Three dots for each protein sample, corresponding to 3  $\mu$ g of protein, were put on the membrane and incubated over night. The membrane was washed twice with TBST 0.05%

and incubated with Blocking Solution for 30 min at r.t. on a shaker. Then, incubation of the membrane with the OC antibody (primary antibody) diluted 1:1000 in Blocking solution for 2 h at r.t. was performed. Subsequently, 4x 5 min washing-steps with TBST 0.05% were followed by the incubation with the secondary antibody (Dako, Glostrup,) diluted 1:1000 in Blocking solution at r.t. for 1 h. After 4x 5 min washing-steps with TBST 0.05%, the immunoreactivity was visualized using Pierce ECL Western Blotting substrate (ThermoScientific, USA). Images were obtained by a MicroChemi Imaging System from Biostep.

#### *A $\beta$ aggregation assay*

A $\beta$  aggregation was determined using a Thioflavin T Beta-Amyloid (1-42) Aggregation Kit (SensoLyte, AnaSpec) according to the manufacturer's instructions. In brief, 900  $\mu$ L of the assay buffer were added to 100  $\mu$ L of Thioflavin to get a 2 mM solution. A $\beta$  peptide was diluted in 1 mL of cold assay buffer and sonicated for 5 min, followed by centrifugation at 10,000 rpm for 5 min at 4 °C. To set up the fibrillation reaction, 10  $\mu$ L of 2 mM Thioflavin were added into each well. Then, 85  $\mu$ L of the A $\beta$  solution and 5  $\mu$ L of the test compounds (NPs) or control were added. As a control for pure Cur, DMSO was used. As control for the NPs, assay buffer was used. The fluorescence intensity was measured at 37°C with an excitation of 440 nm and an emission of 484 nm using a microplate reader (Tecan Infinite PRO 200, Tecan, Switzerland) every 10 min for up to three hours.

#### *Determination of oxidative stress*

Oxidative stress was measured using the CellROX<sup>®</sup> Oxidative Stress detection kit (Thermo Fisher) according to the manufacturer's instructions. CellROX<sup>®</sup> oxidative stress green reagents were used to show possible antioxidant properties of Cur and Cur loaded NPs in



primary hippocampal rat neurons at DIV 14. In brief, CellROX<sup>®</sup> green reagents were added to cells at a concentration of 5  $\mu$ M and cells incubated for 30 min at 37°C. Medium was removed and cells were washed 3 times with PBS. Cells were fixed in 4% PFA/4% sucrose/PBS for 15 min at r.t.. Fluorescence was measured from CellROX<sup>®</sup> green reagents at 520 nm being the oxidized form while CellROX<sup>®</sup> green reagents shows significantly less fluorescence in the reduced state. Oxidative stress was induced *in vitro* to serve as positive control for the CellROX<sup>®</sup> kit and to test for a rescue with Cur. Fenton's reagents were applied overnight on a 24 well plate. 0.5  $\mu$ M of FeCl<sub>2</sub> and 2.5  $\mu$ M of H<sub>2</sub>O<sub>2</sub> were added. The dissociated Fe<sup>2+</sup> ions are able to oxidize while reducing H<sub>2</sub>O<sub>2</sub> to one Hydroxide ion and one Hydroxyl radical ( $\text{Fe}^{2+} + \text{H}_2\text{O}_2 \rightarrow \text{Fe}^{3+} + \text{HO}^- + \text{HO}^{\bullet}$ ).

### *Statistics*

Statistical analysis was performed with SPSS version 20. All data are shown as mean  $\pm$  SEM. For comparisons, one-way analysis of variance (ANOVA) was performed followed by post hoc tests for within group comparisons (Bonferroni test). Statistically significant differences are indicated in the figures by \*  $p \leq 0.05$ , \*\*  $p \leq 0.01$  and \*\*\*  $p \leq 0.001$ .

*Immunocytochemistry* - Acquisition and evaluation of all images were performed under “blinded” conditions. 10 cells of each condition were imaged. All signals within the optic fields were quantified in the following way: Fluorescence images were obtained with an upright Axioscope microscope equipped with a Zeiss CCD camera (16 bits; 1280x1024 ppi) using Axiovision software (Zeiss). Quantification was performed using ImageJ 1.49o.

*Western blot quantification* - Evaluation of bands was performed using ImageJ. Three independent experiments were performed. The individual bands were selected and the integrated density was measured. Bands were normalized to  $\beta$ -actin and the ratios averaged

and tested for significance. For *Dot blot quantification*, signals of individual spots were selected and the integrated density was measured.

## Results

### *Formulation and characterization of novel nanocarriers*

The chemico-physical and technological characterization of samples is reported in **Fig. 1**. All NPs were characterized in terms of size, surface charge, residual amount of surfactant and yield of preparation. All samples, independently of functionalization and/or loading, were featured by the hydrodynamic diameters (*Z*-average) around 200-250 nm and relatively narrow size distributions (polydispersivity, PDI<0.1), favorable for a systemic administration (**Fig. 1A**). Un-modified NPs exhibit high negative value of  $\zeta$ -pot (-22 mV) owing to the exposure of the carboxylic group of PLGA that indicates high electric charge on the surface of the NPs, which is responsible for the strong repulsive forces amongst the particles that prevents their aggregation in water. The functionalization with g7 (g7-NPs) significantly alters the  $\zeta$ -pot value of NPs, reducing the negativity of their surface (about -13 mV); g7-NPs-Cur maintained the surface charge of g7-NPs, suggesting the absence of drug adsorbed on the NP surface. The amount of residual surfactant was less than 8% of the total formulation mass and compatible with parenteral administration (**Fig. 1A**). ESCA analysis, **a versatile tool in identifying the chemical species on the surface of nanoparticles ([Ratner et al., 2009](#))**, was applied. Since all materials forming nanoparticles (PLGA, PVA and Cur) are composed of few atoms (namely C, H and O), the identification of N signal, typical of g7 peptide, are routinely considered as a strong proof of success of the surface engineering procedure. The atomic spectra of the engineered NPs, (g7-NPs and g7-NPs-Cur) in comparison with plain NPs showed N signals indicating that the location of g7 is on the surface of NPs (**Fig. 1B**). AFM images of samples (g7-NPs and g7-NPs-Cur) (**Fig. 1C**) showed a defined and reproducible spherical morphology and smooth surface already observed for un-modified NPs

(data not shown). The AFM diameters were in agreement with PCS data. The presence of residual surfactant could be responsible of some aggregation during the dehydration process (necessary for the analyses). All samples show a yield between 85 and 95%, which can be considered satisfactory.

From a technological point of view, g7-NPs Cur showed high drug loading capacity (LC) of about 3% (w/w) and an encapsulation efficiency (EE) of about 60% (**Fig. 1A**). The release profile of Cur from NPs in simulated physiological condition (PBS buffer added of 50% v/v of serum, **in respect of sink conditions**) is reported in **Fig. 1D**. We observed an initial massive “burst release” (about 60-70%) followed by a second slow release phase. These data suggest the presence of a significant amount of drug in the outer part of the structure, able to rapidly diffuse into the medium. Cur incorporated in the core of NPs was completely diffused within 72 h probably as a consequence of the beginning of NPs degradation.

Additionally, we characterized the g7-NPs-Cur according their photo-physical proprieties (**Fig. 1E**). After excitation at 405 nm, these NPs showed a large emission with a maximum at 510 nm, typical of Cur.

#### ***g7-NPs-Cur show no cell toxicity***

In a first set of experiments, we evaluated whether the novel g7-NPs (loaded/unloaded) exert toxic effects on hippocampal neurons *in vitro*. To that end, we tested the same amount of g7-NPs and g7-NPs-Cur. Fixed amounts of NPs (namely 46, 115 and 230  $\mu\text{g}$  of g7-NPs or g7-NPs-Cur), corresponding to the concentration of 10, 20 and 40  $\mu\text{M}$  of Cur in g7-NPs-Cur were applied to neurons at DIV 13 and the rate of apoptosis and necrosis was measured after 24 h (**Fig. 2A**). Irrespective of the concentration used, no significant increase in apoptotic cells was detected after 24 hours. Selecting a NPs concentration delivering at least 20  $\mu\text{M}$  Cur and various incubation times from 1 h to 7 d, similarly, no increase of apoptotic cells was

visible (**Fig. 2B**). To investigate, whether NPs induce necrosis rather than apoptosis, we applied again concentrations of NPs delivering at least 20  $\mu$ M Cur and evaluated the rate of necrosis after 24 h (**Fig. 2C**) and 7 d (**Fig. 2D**) of treatment using a healthy/necrotic cell detection kit. Necrotic cells were detected by ethidium homodimer III staining and the total number of cells was assessed using Hoechst 33342 labeling all nuclei. No significant increase in necrotic cells was detected. As expected, ethanol (70%), used as positive control, induced a significant increase of necrosis (one-way ANOVA:  $F = 5.419$ ,  $p < 0.001$ ; Bonferroni post hoc  $p = 0.005$  after 24 h and one-way ANOVA:  $F = 3.067$ ,  $p = 0.012$ ; Bonferroni post hoc  $p = 0.023$  after 7d).

### ***g7-NPs-Cur uptake into neurons***

As proof of the affinity of g7-NPs-Cur to neurons, we investigated the cellular uptake by means of fluorescence analysis (**Fig.3**). Since Cur is characterized by large emission spectra which could interfere with signals derived from immunocytochemistry, in order to minimize the interference, we selected as fluorochromes, very strong imaging tools (namely QDs), featured by a very unique and defined signal. Therefore, g7-(QD)-NPs-Cur (see supplementary for information regarding the formulation, Table S1 and Fig S2 for characterization) were incubated with neurons for 3 hr. Data revealed that, on average, 75% (data not shown) of the intracellular nanoparticles co-localized with Clathrin positive signals and we could claim that this output strongly agree with previous published data which described the cellular interaction of g7-NP (unloaded) (Vilella et al., 2015) mediated by clathrin pathways. Moreover, this result is also underlining the fact that the presence of even little amounts of Cur adsorbed onto the NPs surface did not interfere with the efficiency and dynamic of cells interaction.

### ***Increased levels of Cur do not result in cellular toxicity***

As previously evidenced, after exposure of cells to Cur loaded g7-NPs, the g7-NPs are readily taken up into cells. The resulting increase in intracellular and extracellular Cur concentration did not produced significant increase in cell death after 24 h and up to 7 d (Fig. 4A) even if high Cur concentrations (up to 200  $\mu$ M) were used. The most suitable and efficient therapeutic concentration of Cur was indicated to be around 10  $\mu$ M (Goozee et al., 2016) on cellular level. Therefore, in further experiments, this concentration was used. As additional readout, to investigate whether Cur, g7-NPs or g7-NPs-Cur induce mechanisms of cell death not readily detectable on cellular level but on molecular level, we analyzed poly(ADP-ribose) polymerase (PARP). The enzyme caspase-3 can be activated both by extrinsic and intrinsic pathways and contributes to the proteolytic cleavage of key proteins involved in cellular apoptosis, such as the nuclear enzyme PARP (Salvesen, 2002). Thus, the amount of cleaved PARP is indicative of programmed cell death (Virág et al., 2013). However, we could not detect a significant increase in cleaved PARP in hippocampal neurons treated with Cur or g7-NPs after 24 h (Fig. 4B) and 7 d (Fig. 4C) of treatment.

One proposed action of Cur is to act as scavenger of free radicals and thus reduce oxidative stress (Rajeswari, 2006). Therefore, in a next set of experiment, we induced oxidative stress by addition of H<sub>2</sub>O<sub>2</sub> and FeCl<sub>2</sub> (Fenton reaction) (Fig. 4D and 4E). One day after the treatment, oxidative stress was measured by CellRox<sup>®</sup> staining. Neurons showed a significant increase of oxidative stress after treatment compared to untreated cells (one-way ANOVA:  $F = 8.554, p < 0.001$ ). However, cells treated for 30 min and 1 day with Cur did not present such an increase. Cur also acted on untreated control cells hinting towards a reduction of oxidative stress endogenously present in control cultures (Fig. 4D) (Bonferroni post hoc test revealed significant differences between control and control with increased oxidative stress, and all Cur treatment groups  $p < 0.001$ ) Delivery of Cur by g7-NPs had the same protective

effect even after 7 d of treatment (**Fig. 4E**) (one-way ANOVA:  $F = 18.542$ ,  $p < 0.001$ ; Bonferroni post hoc test revealed significant differences between control and control with increased oxidative stress, and control and g7-NPs-Cur treatment groups  $p < 0.001$ ).

#### *Modification of A $\beta$ pathology by Cur loaded g7-NPs in vitro*

Given the promising activity of Cur regarding oxidative stress and A $\beta$  disaggregation ([Yang et al., 2005](#)), in a next set of experiments, we evaluated whether Cur and Cur delivered by g7-NPs indeed **was** able to influence the cellular pathology induced by the presence of A $\beta$  peptides *in vitro*. To that end, we incubated primary hippocampal neurons with 1, 10 and 100  $\mu\text{M}$  of monomeric A $\beta$  for 24 hours and confirmed a significant effect on cell viability after exposure of cells to 10 and 100  $\mu\text{M}$  A $\beta$  (**Fig. 5A**). Ethanol was used as positive control (one-way ANOVA:  $F = 6.139$ ,  $p < 0.001$ ; Bonferroni post hoc test revealed significant differences between control vs. EtOH control  $p = 0.003$ ; control vs. A $\beta_{10\mu\text{M}}$   $p = 0.07$ ; control vs. A $\beta_{100\mu\text{M}}$   $p = 0.0002$ ). Next, we investigated whether this effect on cell health can be modified by additional exposure of cells to Cur and g7-NPs-Cur (**Fig. 5B**). Our results show that after 7 d of treatment, exposure of cells to A $\beta$  again leads to a reduction in cell health. The addition of Cur or g7-NPs-Cur to these cultures partly restores cell health (seen as trend) (**Fig. 5B**).

To answer the question, whether a positive effect of Cur is realized via altered A $\beta$  aggregation, we again treated neurons with 100  $\mu\text{M}$  A $\beta$  and Cur and Cur delivering g7-NPs. After 7 d, the cell culture medium containing extracellular A $\beta$  aggregates was removed and analyzed by native Western Blot and anti-A $\beta$  labeling (**Fig. 5C**). A reduction in higher order A $\beta$  aggregates was visible in conditions with exposure to Cur.

To confirm the reduction in A $\beta$  aggregates by g7-NPs-Cur, we performed a thioflavin T based ELISA assay. An increase of fluorescence signal is correlated with an increase of A $\beta_{42}$  fibril formation. As control, inhibitors of A $\beta$  aggregation (Morin/Phenol Red) were used (**Fig. 5D**).

The results show that co-incubation of A $\beta$  with g7-NPs-Cur leads to a significant reduction of the observed A $\beta$  aggregation and disaggregation was observed (one-way ANOVA:  $F = 166.839$ ,  $p < 0.0001$ ; Bonferroni post hoc test revealed significant differences between all groups  $p < 0.001$ ). Moreover, unloaded g7-NPs increased A $\beta$  aggregation at short time. This finding is not surprising since, as described by Radic and coworkers ([Radic et al., 2015](#)), nanoparticles, in function of both their properties and the experimental conditions (concentration, ratio with A $\beta$  peptides etc) could be able to initially attract peptides promoting A $\beta$  aggregation onto the NP surface due to increased local protein concentration on the surface and destabilization of the folded state. However, at longer time-points, a further increase in NPs-peptide attraction could lead to a decrease of amyloid fibrils stability and to a reduction of their lateral diffusion on the NP surface, necessary for peptide conformational changes and self-association, thus prohibiting amyloid aggregation.

To further verify these findings, we used A $\beta$  conformation dependent antibodies (OC antibody) that specifically recognize distinct assembly states of amyloids, including prefibrillar oligomers and fibrils. The OC antibody is able to recognize fibrillary oligomers that are immunologically distinct from prefibrillar oligomers ([Kayed et al., 2007](#)). Dot blot analysis shows the presence of fibrillary oligomers in all cultures exposed to A $\beta$ . As indicated by the previous results, the immune-reactive signal of OC antibody is significantly reduced by treatment with Cur and g7-NPs-Cur ([Fig. 5E](#)) again hinting towards a reduced aggregation and/or disaggregation of A $\beta$  (one-way ANOVA:  $F = 91.639$ ,  $p < 0.0001$ ; Bonferroni post hoc test revealed significant differences between all groups and the Control  $p < 0.001$ ; Moreover a significant difference is detected between A $\beta$  and A $\beta$  + Cur  $p = 0.049$ , and A $\beta$  + g7-NPs-Cur  $p < 0.001$ ).

Further, we detected that the number of A $\beta$  positive signals per area was significantly reduced in cultures treated with Cur loaded g7-NPs 7d after incubation with 10  $\mu$ M of monomeric A $\beta$

and g7-NPs (**Fig. 5F**) (one-way ANOVA:  $F = 34.493$ ,  $p < 0.0001$ ; Bonferroni post hoc test revealed significant differences between  $A\beta$  and  $A\beta + \text{Cur}$   $p < 0.001$ , and  $A\beta + \text{g7-NPs-Cur}$   $p < 0.001$ ).

The NF- $\kappa$ B (nuclear factor 'kappa-light-chain-enhancer' of activated B-cells) pathway is important for the expression of many genes involved in inflammatory response and the constitutive activation of the pathway is associated with AD ([Yamamoto and Gaynor, 2004](#)). NF- $\kappa$ B is controlled by a family of inhibitory proteins known as I $\kappa$ B, which include I $\kappa$ B $\alpha$ , I $\kappa$ B $\beta$ , I $\kappa$ B $\epsilon$  and I $\kappa$ B $\gamma$ . I $\kappa$ B thereby inhibits NF- $\kappa$ B. Therefore, new therapeutic targets that prevent the aberrant activation of NF- $\kappa$ B might be promising in AD. As it was previously reported that Cur analogs act as NF- $\kappa$ B inhibitor ([Kasinski et al., 2008](#)), and that Cur decreases the phosphorylation of I $\kappa$ B, we next assessed the ability of g7-NPs-Cur to influence I $\kappa$ B. To that end, we measured the signal intensity of I $\kappa$ B staining to generate an indirect read-out of I $\kappa$ B influences on NF- $\kappa$ B (**Fig. 4G**). Our results show that the fluorescence intensity of I $\kappa$ B immunoreactive signals is decreased after treatment of neurons with  $A\beta$ . In contrast, application of Cur as solution or delivered by g7-NPs-Cur was able to prevent this decrease (one-way ANOVA:  $F = 4.242$ ,  $p < 0.001$ ; Bonferroni post hoc test revealed significant differences between  $A\beta$  and  $A\beta$  plus g7-NPs-Cur treated cells  $p = 0.002$ , and between  $A\beta$  plus g7-NPs and  $A\beta$  plus g7-NPs-Cur treated cells  $p = 0.021$ ). The level of I $\kappa$ B immunoreactivity was even higher (seen as trend) as in controls upon treatment with Cur and g7-NPs-Cur independent of the presence of  $A\beta$  hinting towards a general mechanism of Cur. Finally, as the loss of synapses may be the best cellular correlate to the cognitive impairments observed in AD patients, we assessed the ability of g7-NPs-Cur to prevent the decrease in synapse density observed after exposure of neurons to  $A\beta$  ([Grabrucker et al., 2011b](#)). The mean number of synapses (Bassoon immunoreactive puncta) per dendrite length was measured 7 d after treatment with 10  $\mu$ M  $A\beta$  (**Fig. 5H**). As expected, a reduction can be



observed in neurons exposed to A $\beta$ . Interestingly, although not significant, a trend towards a rescue is observed in neurons treated with g7-NPs-Cur.

## Discussion

Extracellular and intracellular protein aggregates are disruptive for synaptic function and cell health and are broadly held to be the major culprit of brain dysfunction underlying AD. Developing treatment strategies aiming to reduce protein aggregation and propagation are therefore highly desired goals.

The use of innovative drug delivery systems engineered on their surface to pass the BBB offers a non-invasive tool for CNS drug delivery. Previously, we have yet demonstrated that surface engineered NPs made of a FDA-approved polymer are able to both stabilize active compounds with different molecular weights and to cross the BBB after systemic administration in wild-type and knockout rodents ([Grabrucker et al., 2016](#), [Salvalaio et al., 2016](#), [Valenza et al., 2015](#)). Here, we developed a new generation of NPs potentially able to modify A $\beta$  aggregates within the brain (g7-NPs-Cur). By that, we delivered Cur, a novel compound identified to be able to interfere with A $\beta$  aggregation. Our *in vitro* data shows that g7-NPs-Cur are non-toxic for cells in concentrations delivering 10  $\mu$ M Cur. Moreover, g7-NPs-Cur are able to reduce oxidative stress and to inhibit A $\beta$  aggregation as well as to promote A $\beta$  disaggregation more efficiently with respect to un-loaded free Cur. Taken together, our data clearly demonstrated a superior ability of g7-loaded nanoparticles to increase the cellular affinity of the active for neuronal cells.

Interestingly, Cur binds to copper and zinc ions, but only weakly to zinc ions ([Baum and Ng, 2004](#)) suggesting that Cur is able to decrease inflammatory damage by preventing metal induction of NF- $\kappa$ B ([Mishra and Palanivelu, 2008](#)) and Cur was reported to decrease I $\kappa$ B phosphorylation that leads to a reduced inhibition of NF- $\kappa$ B. Here, we were further able to

confirm a modulatory role of Cur delivered by NPs on the I $\kappa$ B complex. The loss of I $\kappa$ B that was observed in presence of A $\beta$  aggregates was absent in cells treated with g7-NPs-Cur. Thus, it is indeed possible that Cur ameliorates inflammatory processes in AD brains.

In conclusion, reduced oxidative stress, inflammation and plaque load are the major outcomes observed in *in vitro* experiments confirming that the g7-NPs-Cur provided an efficient delivery for loaded Cur and proved a promising carrier candidate **for treating AD**.

**Although further conclusions can be drawn only after a complete *in vivo* study in AD animal models, the results of this preliminary study suggest the potential role of surface modified loaded nanoparticles in stabilizing Cur, potentially solving the problem of administration and potentiating the effect of Cur against A $\beta$  related toxicity.**

## **Acknowledgments**

JK is a member of the International Graduate School of Molecular Medicine at Ulm University. This research was partially supported by UNIMORE grant FAR 2014 (PI Prof. Maria Angela Vandelli) and UNIMORE grant FAR 2014 (PI Prof. Giovanni Tosi).

## **Declaration of competing interests**

The authors declare that they have no competing interests.

## **Literature**

Abbott, N.J., Patabendige, A.A.K., Dolman, D.E.M., Yusof, S.R., Begley D.J., 2010. Structure and Function of the Blood–brain Barrier. *Neurobiol. Dis.* 37, 13-25.

Anand, P., Kunnumakkara, A.B., Newman, R.A., Aggarwal, B.B., 2007. Bioavailability of curcumin: problems and promises. *Mol Pharm.* 4, 807-818.

Baum, L., Ng, A., 2004. Curcumin interaction with copper and iron suggests one possible mechanism of action in Alzheimer's disease animal models. *J. Alzheimers Dis.* 6, 367-377.

Bondioli, L., Costantino, L., Ballestrazzi, A., Lucchesi, D., Boraschi, D., Pellati, F., Benvenuti, S., Tosi, G., Vandelli, M.A., 2010. PLGA nanoparticles surface decorated with the sialic acid, N-acetylneuraminic acid. *Biomaterials* 31, 3395–3403.

Butterfield, D.A., 1997. Beta-Amyloid-Associated Free Radical Oxidative Stress and Neurotoxicity: Implications for Alzheimer's Disease. *Chem. Res. Toxicol.* 10, 495–506.

Butters, N., Granholm, E., Salmon, D. P., Grant, I., & Wolfe, J., 1987. Episodic and semantic memory: a comparison of amnesic and demented patients. *J. Clin. Exp. Neuropsychol.* 9, 479–497.

Costantino, L., Gandolfi, F., Tosi, G., Rivasi, F., Vandelli, M.A., Forni, F., 2005. Peptidederivatized biodegradable nanoparticles able to cross the blood-brain barrier. *J. Control. Release* 108, 84 – 96.

Esatbeyoglu, T., Huebbe, P., Ernst, I.M.A., Chin, D., Wagner, A.E., Rimbach, G., 2012. Curcumin - Vom Molekül Zur Biologischen Wirkung. *Angewandte Chemie* 124, 5402–5427.

Gallo, J.M., Noble, W., Martin, T.R., 2007. RNA and protein-dependent mechanisms in tauopathies: consequences for therapeutic strategies. *Cell. Mol. Life Sci.* 64, 1701-1714.

Goozee, K.G., Shah, T.M., Sohrabi, H.R., Rainey-Smith, S.R., Brown, B., Verdile, G., Martins, R.N., 2016. Examining the potential clinical value of curcumin in the prevention and diagnosis of Alzheimer's disease. *Br. J. Nutr.* 115, 449-465.

Grabrucker, A., Vaida, B., Bockmann, J., Boeckers, T.M., 2009. Synaptogenesis of hippocampal neurons in primary cell culture. *Cell. Tissue Res.* 338, 333-341.

Grabrucker, A.M., Garner, C.C., Boeckers, T.M., Bondioli, L., Ruozi, B., Forni, F., Vandelli, M.A., Tosi, G., 2011a. Development of novel Zn<sup>2+</sup> loaded nanoparticles designed for cell type targeted drug release in CNS neurons: in vitro evidences. *Plos One* 6, e17851

Grabrucker, A.M., Ruozi, B., Belletti, D., Pederzoli, F., Forni, F., Vandelli, M.A., Tosi, G., 2016. Nanoparticle transport across the blood brain barrier. *Tissue Barriers* 4, e1153568.

Grabrucker, A.M., Schmeisser, M.J., Udvardi, P.T., Arons, M., Schoen, M., Woodling, N.S., Andreasson, K.I., Hof, P.R., Buxbaum, J.D., Garner, C.C., Boeckers, T.M., 2011b. Amyloid beta protein-induced zinc sequestration leads to synaptic loss via dysregulation of the ProSAP2/Shank3 scaffold. *Mol. Neurodegener.* 6: 65.

Hussain, Z., Thu, H.E., Ng, S.F., Khan, S., Katas, H., 2017. Nanoencapsulation, an efficient and promising approach to maximize wound healing efficacy of curcumin: A review of new trends and state-of-the-art. *Colloids Surf B Biointerfaces*. doi: 10.1016/j.colsurfb.2016.11.036.

Joshi, D.P., Lan-Chun-Fung, Y.L., Pritchard, J.G., 1979. Determination of poly(vinyl alcohol) via its complex with boric acid and iodine. *Anal. Chim Acta* 104, 153–160.

Kasinski, A.L., Du, Y., Thomas, S.L., Zhao, J., Sun, S.Y., Khuri, F.R., Wang, C.Y., Shoji, M., Sun, A., Snyder, J.P., Liotta, D., Fu, H., 2008. Inhibition of I $\kappa$ B kinase-nuclear factor- $\kappa$ B signaling pathway by 3,5-bis(2-fluorobenzylidene)piperidin-4-one (EF24), a novel monoketone analog of curcumin. *Mol. Pharmacol.* 74, 654-661.

Kayed, R., Head, E., Sarsoza, F., Saing, T., Cotman, C.W., Necula, M., Margol, L., Wu, J., Breydo, L., Thompson, J.L., Rasool, S., Gurlo, T., Butler, P., Glabe, C.G., 2007. Fibril specific, conformation dependent antibodies recognize a generic epitope common to amyloid fibrils and fibrillar oligomers that is absent in prefibrillar oligomers. *Mol. Neurodegener.* 2: 18.

Kumar, S., Walter, J., 2011. Phosphorylation of Amyloid Beta (A $\beta$ ) Peptides - a Trigger for Formation of Toxic Aggregates in Alzheimer's Disease. *Aging* 3, 803–812.

Lazar, A.N., Mourtas, S., Youssef, I., Parizot, C., Dauphin, A., Delatour, B., Antimisiaris, S.G., Duyckaerts, C., 2013. Curcumin-conjugated nanoliposomes with high affinity for A $\beta$  deposits: possible applications to Alzheimer disease. *Nanomedicine.* 9, 712-721.

Lin, J.K., Chen, Y.C., Huang Y.T., Lin-Shiau. S.Y., 1997. Suppression of Protein Kinase C and Nuclear Oncogene Expression as Possible Molecular Mechanisms of Cancer Chemoprevention by Apigenin and Curcumin. *J. Cell. Biochem.* 67, 39–48.

Mainardes, R.M., Evangelista, R.C., 2005. Praziquantel-loaded PLGA nanoparticles: preparation and characterization. *J. Microencapsul.* 22, 13–24.

Mathew, A., Fukuda, T., Nagaoka, Y., Hasumura, T., Morimoto, H., Yoshida, Y., Maekawa, T., Venugopal, K., Kumar, D.S., 2012. Curcumin loaded-PLGA nanoparticles conjugated with Tet-1 peptide for potential use in Alzheimer's disease. *PLoS One*. 7, e32616.

Mishra, S., Palanivelu, K., 2008. The effect of curcumin (turmeric) on Alzheimer's disease: An overview. *Ann. Indian. Acad. Neurol.* 11, 13-19.

Mulik, R.S., Mönkkönen, J., Juvonen, R.O., Mahadik, K.R., Paradkar, A.R., 2010. ApoE3 mediated poly(butyl) cyanoacrylate nanoparticles containing curcumin: study of enhanced activity of curcumin against beta amyloid induced cytotoxicity using in vitro cell culture model. *Mol Pharm.* 7, 815-825.

Mundargi, R.C., Babu, V.R., Rangaswamy, V., Patel, P., Aminabhavi, T.M., 2008. Nano/micro technologies for delivering macromolecular therapeutics using poly(D, L-lactide-co-glycolide) and its derivatives. *J. Control. Release* 125, 193 – 209.

Perl, D.P., 2010. Neuropathology of Alzheimer's disease. *Mt Sinai J. Med.* 77, 32-42.

Radic, S., Davis, T.P., Ke, P.C., Ding, F., 2015. Contrasting effects of nanoparticle–protein attraction on amyloid aggregation, *RSC Adv.* 5, 105489-105498.

Rajeswari, A., 2006. Curcumin protects mouse brain from oxidative stress caused by 1-methyl-4-phenyl-1,2,3,6-tetrahydropyridine. *Eur. Rev. Med. Pharmacol. Sci.* 10, 157-161.

Ray, B., Lahiri, D.K., 2009. Neuroinflammation in Alzheimer's Disease: Different Molecular Targets and Potential Therapeutic Agents Including Curcumin. *Curr Opin Pharmacol* 9, 434–444.

Ratner, B. D. and Castner, D. G. (2009) Electron Spectroscopy for Chemical Analysis, in Surface Analysis - The Principal Techniques, 2nd Edition (eds J. C. Vickerman and I. S. Gilmore), John Wiley & Sons, Ltd, Chichester, UK.

Salvalaio, M., Rigon, L., Belletti, D., D'Avanzo, F., Pederzoli, F., Ruozi, B., Marin, O., Vandelli, M.A., Forni, F., Scarpa, M., Tomanin, R., Tosi, G., 2016. Targeted Polymeric Nanoparticles for Brain Delivery of High Molecular Weight Molecules in Lysosomal Storage Disorders. *PLoS One* 11, e0156452.

Salvesen, G.S., Duckett, C.S., 2002. Iap Proteins : Blocking the Road To Death ' S Door. *Nat. Rev. Mol. Cell Biol.* 3, 401-410.

Schellenberg, G.D., Montine, T.J., 2012. The genetics and neuropathology of Alzheimer's disease. *Acta Neuropathol.* 124, 305-323.

Schmeisser, M.J., Ey, E., Wegener, S., Bockmann, J., Stempel, A.V., Kuebler, A., Janssen, A.L., Udvardi, P.T., Shibani, E., Spilker, C., Balschun, D., Skryabin, B.V., Dieck, St., Smalla, K.H., Montag, D., Leblond, C.S., Faure, P., Torquet, N., Le Sourd, A.M., Toro, R., Grabrucker, A.M., Shoichet, S.A., Schmitz, D., Kreutz, M.R., Bourgeron, T., Gundelfinger, E.D., Boeckers, T.M., 2012. Autistic-like behaviours and hyperactivity in mice lacking ProSAP1/Shank2. *Nature* 486, 256-260.

Subramani, P.A., Panati, K., Narala, V.R., 2017. Curcumin Nanotechnologies and Its Anticancer Activity. *Nutr Cancer*. 69, 381-393.

Tosi, G., Costantino, L., Rivasi, F., Ruozi, B., Leo, E., Vergoni, A.V., Tacchi, R., Bertolini, A., Vandelli, M.A., Forni, F., 2007. Targeting the central nervous system: in vivo experiments with peptide-derivatized nanoparticles loaded with Loperamide and Rhodamine-123. *J. Control. Release* 122, 1 – 9.

Tosi, G., Costantino, L., Ruozi, B., Forni, F., Vandelli, M.A., 2008. Polymeric nanoparticles for the drug delivery to the central nervous system. *Expert Opin. Drug Deliv.* 5, 155 – 174.

Tosi, G., Fano, R.A., Bondioli, L., Badiali, L., Benassi, R., Rivasi, F., Ruozi, B., Forni, F., Vandelli, M.A., 2011. Investigation on mechanisms of glycopeptide nanoparticles for drug delivery across the blood-brain barrier. *Nanomedicine* 6, 423 – 436.

Tosi, G., Ruozi, B., Belletti, D., Vilella, A., Zoli, M., Vandelli, M.A., Forni, F., 2013. Brain-targeted polymeric nanoparticles: in vivo evidences after different routes of administration in rodents. *Nanomedicine UK* 8, 1373-1383.

Tosi, G., Vergoni, A.V., Ruozi, B., Bondioli, L., Badiali, L., Rivasi, F., Costantino, L., Forni, F., Vandelli, M.A., 2010. Sialic acid and glycopeptides conjugated PLGA nanoparticles for central nervous system targeting: in vivo pharmacological evidence and biodistribution. *J. Control. Release* 145, 49 – 57.



Valenza, M., Chen, J.Y., Di Paolo, E., Ruozi, B., Belletti, D., Ferrari Bardile, C., Leoni, V., Caccia, C., Brilli, E., Di Donato, S., Boido, M.M., Vercelli, A., Vandelli, M.A., Forni, F., Cepeda, C., Levine, M.S., Tosi, G., Cattaneo, E., 2015. Cholesterol-loaded nanoparticles ameliorate synaptic and cognitive function in Huntington's disease mice. *EMBO Mol. Med.* 7, 1547-1564.

Vassar, R., Bennett, B.D., Babu-Khan, S., Kahn, S., Mendiaz, E.A., Denis, P., Teplow, D.B., Ross, S., Amarante, P., Loeloff, R., Luo, Y., Fisher, S., Fuller, J., Edenson, S., Lile, J., Jarosinski, M.A., Biere, A.L., Curran, E., Burgess, T., Louis, J.C., Collins, F., Treanor, J., Rogers, G., Citron, M., 1999. Beta-Secretase Cleavage of Alzheimer's Amyloid Precursor Protein by the Transmembrane Aspartic Protease BACE. *Science* 286, 735–741.

Vergoni, A.V., Tosi, G., Tacchi, R., Vandelli, M.A., Bertolini, A., Costantino, L., 2009. Nanoparticles as Drug Delivery Agents Specific for CNS: In Vivo Biodistribution. *Nanomedicine* 5, 369–77.

Vilella, A., Ruozi B., Belletti, D., Pederzoli F., Galliani M., Semeghini V., Forni F., Zoli M., Vandelli M.A., Tosi G., 2015. Endocytosis of Nanomedicines: The Case of Glycopeptide Engineered PLGA Nanoparticles. *Pharmaceutics*. 7, 74–89.

Virag, L., Robaszkiewicz, A., Rodriguez-Vargas, J. M., Oliver, F. J., 2013. Poly(ADP-ribose) signaling in cell death. *Mol. Aspects Med.* 34, 1153–1167.

Yamamoto, Y., Gaynor, R.B., 2004. IκB kinases: key regulators of the NF-κB pathway. *Trends Biochem. Sci.* 29, 72-79.

Yang, F., Lim, G.P., Begum, A.N., Ubeda, O.J., Simmons, M.R., Ambegaokar, S.S., Chen, P.P., Kaye, R., Glabe, C.G., Frautschi, S.A., Cole, G.M., 2005. Curcumin inhibits formation of amyloid beta oligomers and fibrils, binds plaques, and reduces amyloid in vivo. *J. Biol. Chem.* 280, 5892-5901.

## Figure legends:

**Figure 1: Characterization of NP samples.** (A) Chemico-physical parameters of samples. Z-Average, PDI (polydispersivity index) and  $\zeta$ -pot (Zeta Potential) of NPs in distilled water after the purification process. The percentage of encapsulation efficiency (EE) was determined as the ratio of the encapsulated out of the total (encapsulated + free) drug per cent (%). The percentage of loading capacity (LC) was expressed as the ratio of the encapsulated drug out of the total mass (encapsulated drug + lipids and/or polymer) per cent. The percentage of Yield was expressed as the ratio of the recovered freeze-dried sample (excluded residual PVA) out of the total mass weighted (polymer and drug) per cent. ESCA: Electron Spectroscopy for Chemical Analysis. All the values represent the means of at least three experiments; standard deviation (SD) in parentheses. (B) Examples of spectra recovered by ESCA. (C) AFM images of samples (g7-NPs and g7-NPs-Cur) were analyzed to obtain the height profile and diameter of particles. (D) Profile of drug release for g7-NPs-Cur obtained in simulated physiological condition (PBS buffer added of 50% v/V of serum). (E) Photo physical characterization of g7-NPs-Cur obtained by confocal microscopy after excitation at 405 nm.

**Figure 2: Evaluation of possible cell toxicity of NPs.** (A) At DIV 13, cells were incubated with three different concentrations of loaded nanoparticles ranging from 46 to 230  $\mu\text{g}$  for 24 hours. (B) Incubation of neurons with 115  $\mu\text{g}$  of g7 NPs-Cur for 1 h, 24 h and 7 d. (C,D) Healthy/necrotic percentage of cells measured after 24 h (C) or 7 d (D) using a cell detection kit. Results were normalized against the untreated control. Ethanol (70%) was used as positive control. All analyses were performed by investigating 10 optic fields of view (n=10).

**Figure 3: QDs modified Cur loaded NPs are taken up into cells.** At DIV 13, cells were incubated with 20  $\mu\text{g}$  of labeled g7-NPs-Cur (g7-(QDs)-NPs-Cur) for 3 hours. Hippocampal neurons were stained for DAPI (blue) (A) and clathrin (green) (B). g7-(QDs)-NPs-Cur were visualized as red spot (C). Neurons were visualized by Map2 staining (cyan) (D). E shows a merged image of signals.

**Figure 4: Increased levels of Cur do not result in cellular toxicity.** (A) Toxicity after treatment with Cur after 24 h or 7 d. All analyses were performed by investigating 10 optic fields of view (n=10). (B, C) Western Blot and the expression/cleavage of Parp detected in hippocampal neurons treated with 10  $\mu\text{M}$  of encapsulated Cur for 24 h (B) and 7 d (C). (D-E) Oxidative stress was induced by addition of  $\text{H}_2\text{O}_2$  and  $\text{FeCl}_2$  (Fenton

reaction). Oxidative stress after treatment with Cur (D) or g7 nanoparticles (E) was measured by CellRox staining.

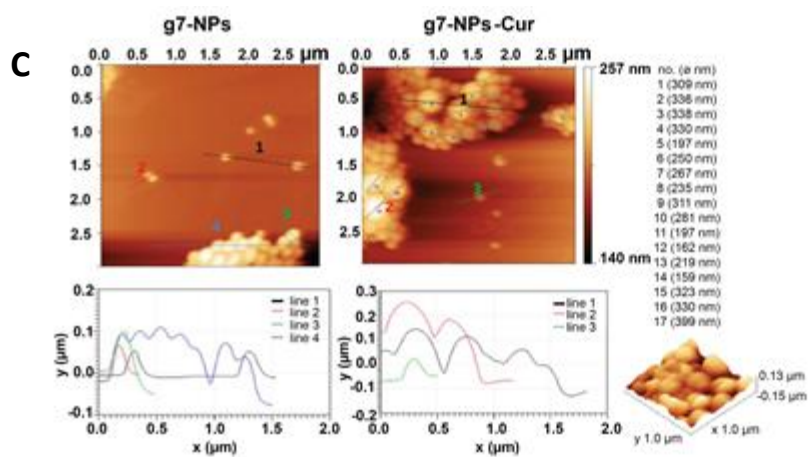
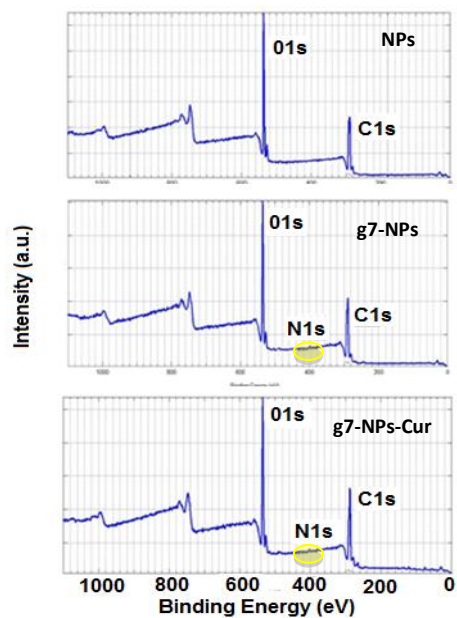
**Figure 5: Modification of A $\beta$  pathology by Cur loaded g7-NPs *in vitro*.** (A) Primary hippocampal neurons were incubated with 1, 10 and 100  $\mu$ M of monomeric A $\beta$  for 24 hours. Ethanol was used as positive control. All values were normalized to the untreated control. (B) cell viability of neurons treated with 46  $\mu$ g of Nanoparticles corresponding to 10  $\mu$ M of loaded Cur for 7 d. The cells were additionally exposed to 10  $\mu$ M A $\beta$ . (C) Western blot of extracellular A $\beta$  aggregates after 7 d of treatment with Cur free or loaded into g7-NPs-Cur. (D) Thioflavin T ELISA assay. (E) Dot blot analysis-of the OC antibody in supernatants of cell cultures exposed to A $\beta$ . OC signals were normalized to Ponceau S signals of the corresponding dot. Analysis was performed in triplicates. (F) Primary hippocampal neurons were incubated with 10  $\mu$ M of monomeric A $\beta$  and 46 $\mu$ g of Nanoparticles to obtain a final concentration of 10  $\mu$ M Cur for 7 d. A $\beta$  aggregates were visualized by immunocytochemistry (green signal). Neurons were stained for MAP2. The number of A $\beta$  positive signals per area was measured in ten optic fields per condition. (G) The fluorescence intensity of I $\kappa$ B immunoreactive signals was measured in at least 10 cells per group. (H) The mean number of synapses per dendrite length (primary and secondary dendrite) was measured 7 d after treatment with 10  $\mu$ M of monomeric A $\beta$ . Synapses were visualized by staining for Bassoon.

Figure 1  
Figure 1

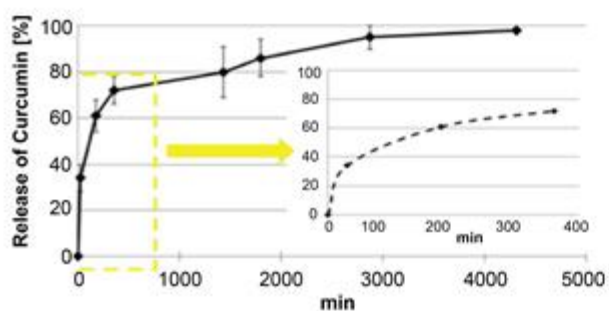
**A**

Sample	NPs	g7-NPs	g7-NPs-Cur
Z-Average (nm $\pm$ S.D.)	199 (9)	202 (6)	204 (10)
PDI ( $\pm$ S.D.)	0.07 (0.02)	0.03 (0.02)	0.07 (0.02)
$\zeta$ -pot (mV $\pm$ S.D.)	-22 (5)	-13 (1)	-13 (2)
PVA (%) ( $\pm$ S.D.)	7 (2)	6 (2)	5 (3)
LC (%) ( $\pm$ S.D.)			3.1 (0.8)
EE (%) ( $\pm$ S.D.)			60 (6)
Yield (%) ( $\pm$ S.D.)	87 (2)	88 (3)	97 (2)
ESCA (C%, O%, N%)	77 (2) 22 (4) /	65 (3) 34 (2) 0.7 (0.1)	67 (3) 32 (3) 0.5 (0.1)

**B**



**D**



**E**

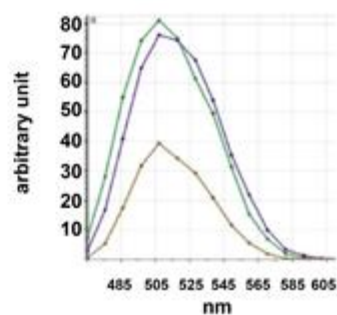


Figure 2

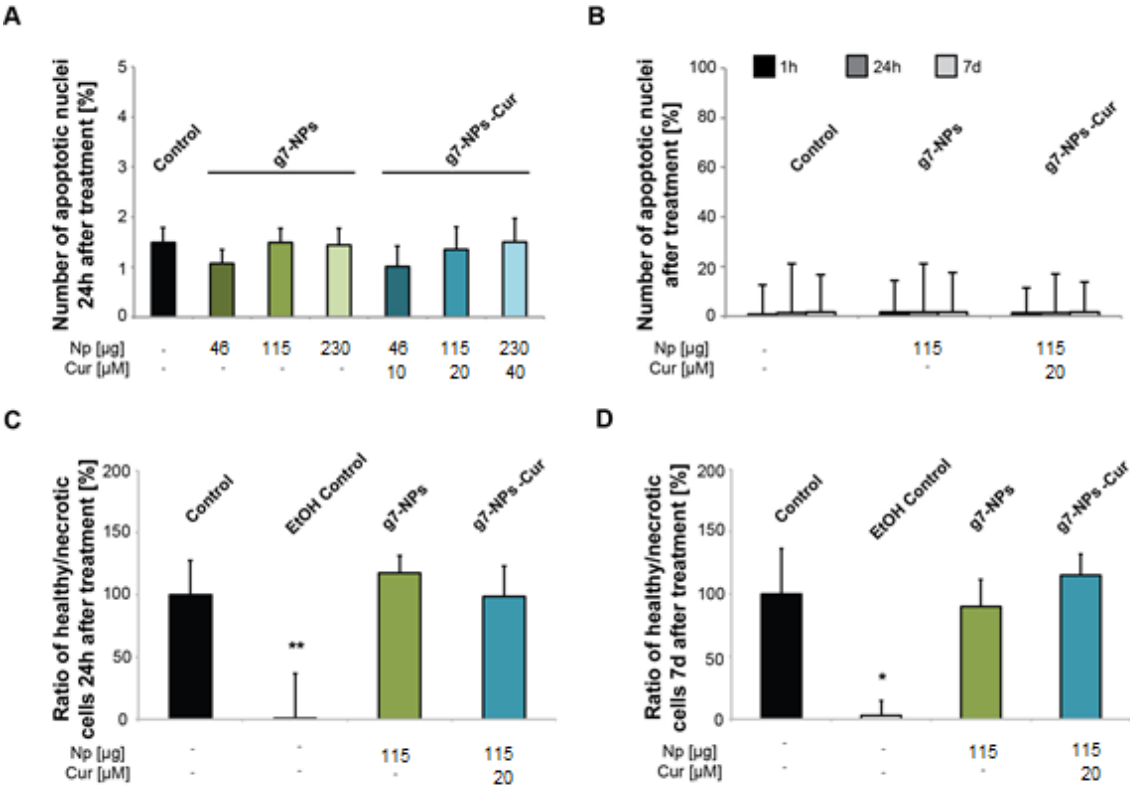


Figure 3

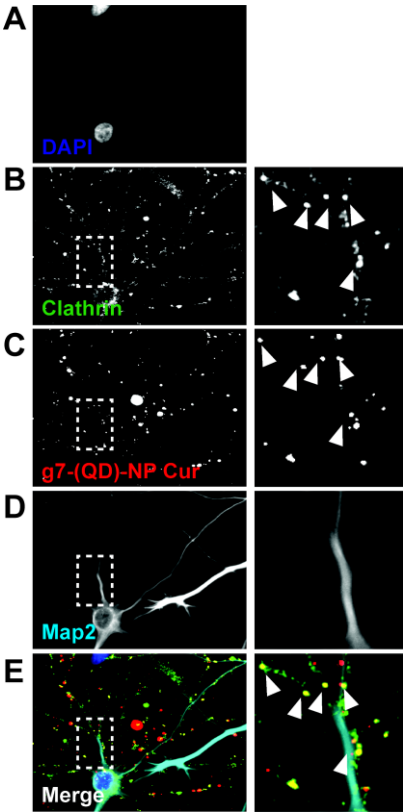


Figure 4

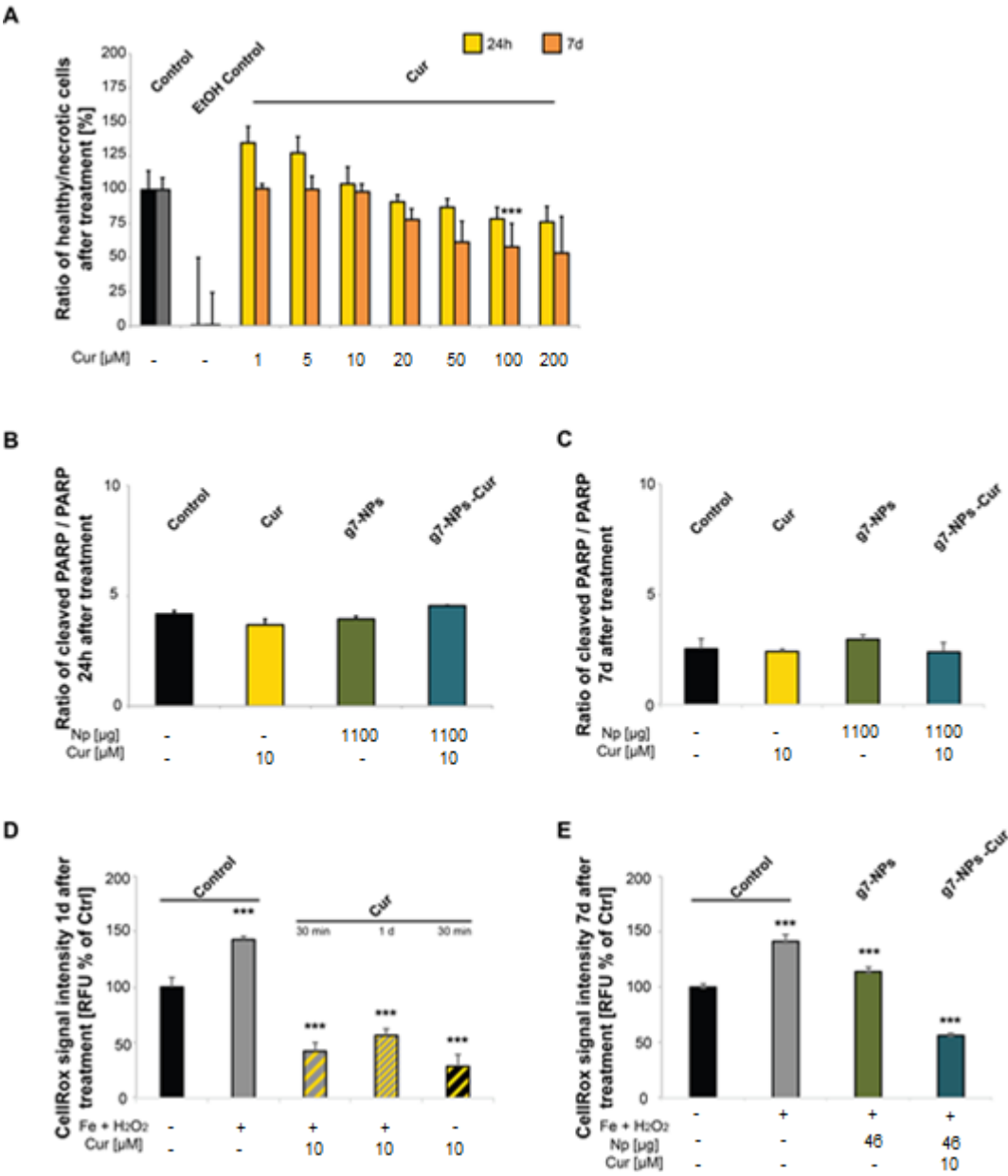




Figure 5

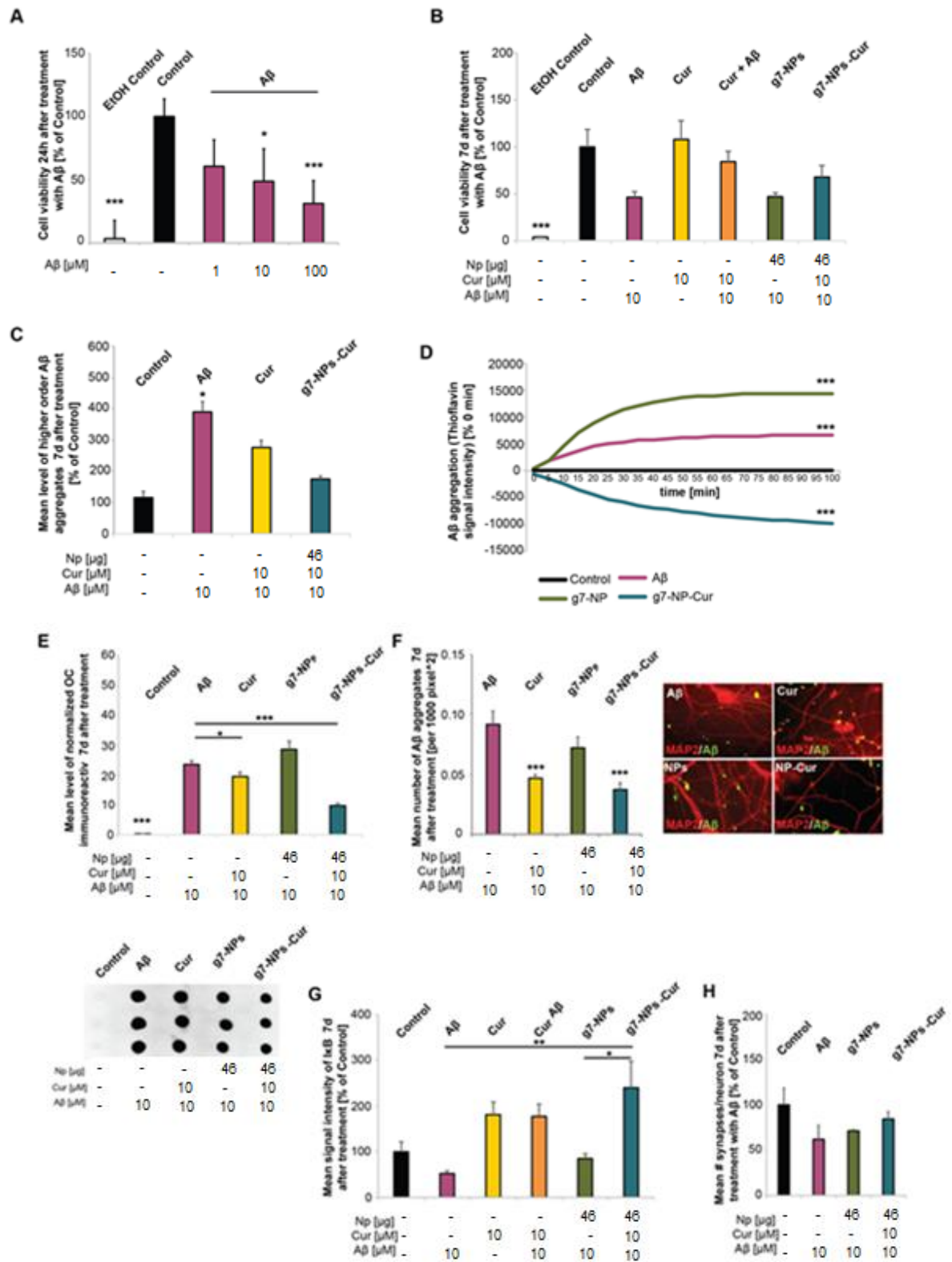
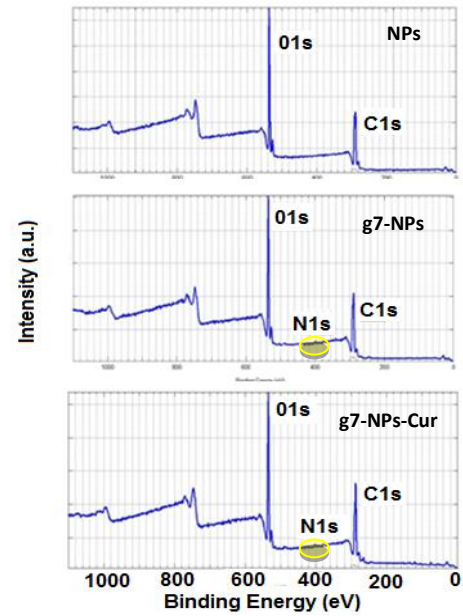


Figure 1

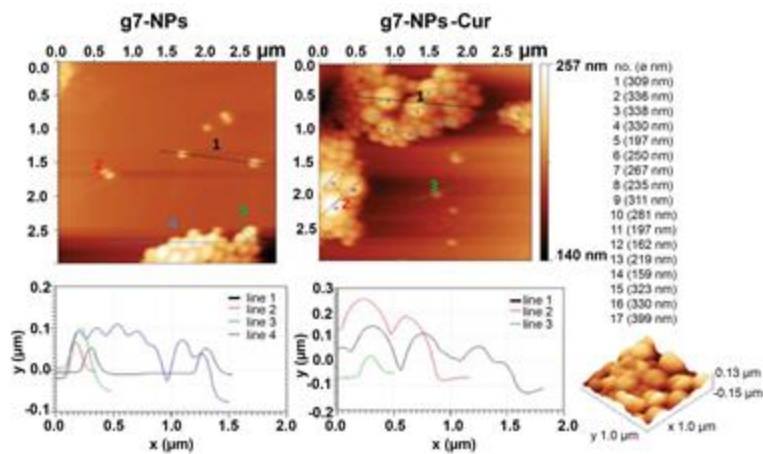
A

Sample	NPs	g7-NPs	g7-NPs-Cur
Z-Average (nm $\pm$ S.D.)	199 (9)	202 (6)	204 (10)
PDI ( $\pm$ S.D.)	0.07 (0.02)	0.03 (0.02)	0.07 (0.02)
$\zeta$ -pot (mV $\pm$ S.D.)	-22 (5)	-13 (1)	-13 (2)
PVA (%) ( $\pm$ S.D.)	7 (2)	6 (2)	5 (3)
LC (%) ( $\pm$ S.D.)			3.1 (0.8)
EE (%) ( $\pm$ S.D.)			60 (6)
Yield (%) ( $\pm$ S.D.)	87 (2)	88 (3)	97 (2)
ESCA (C%, O%, N%)	77 (2) 22 (4) /	65 (3) 34 (2) 0.7 (0.1)	67 (3) 32 (3) 0.5 (0.1)

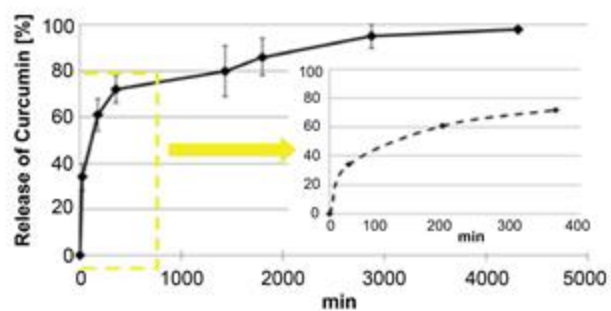
B



C



D



E

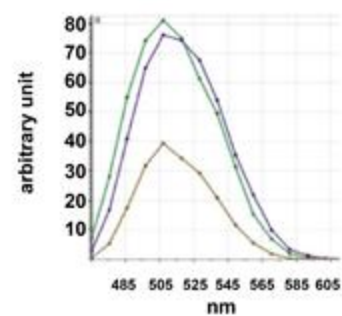


Figure 2

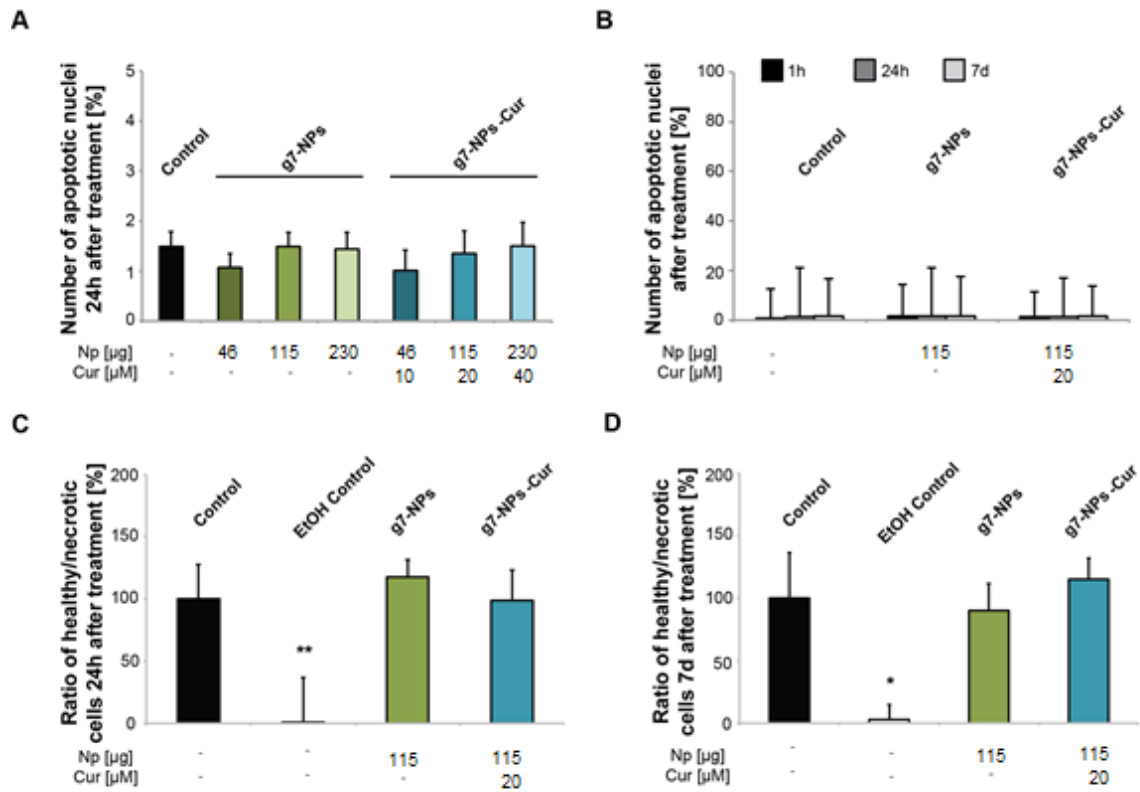


Figure 3

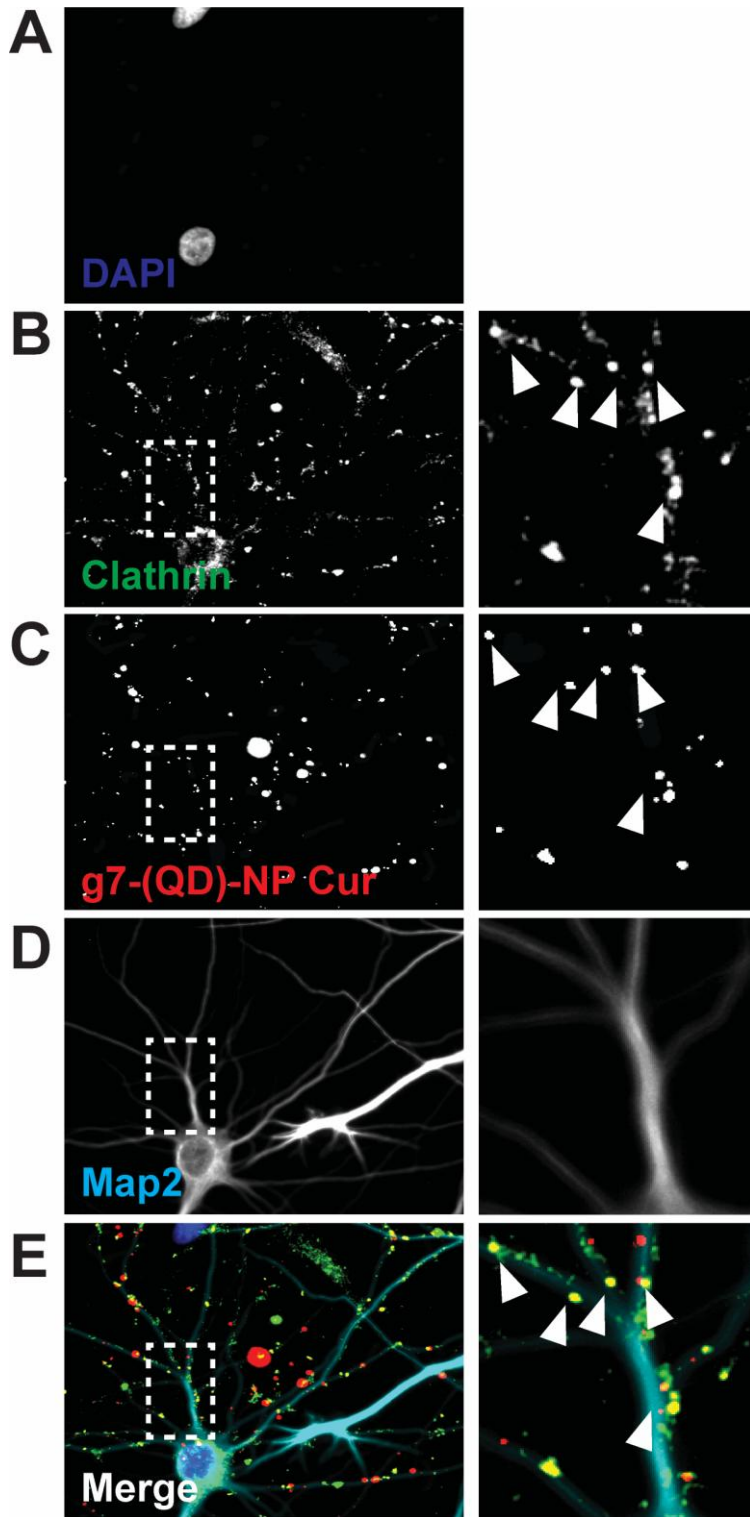


Figure 4

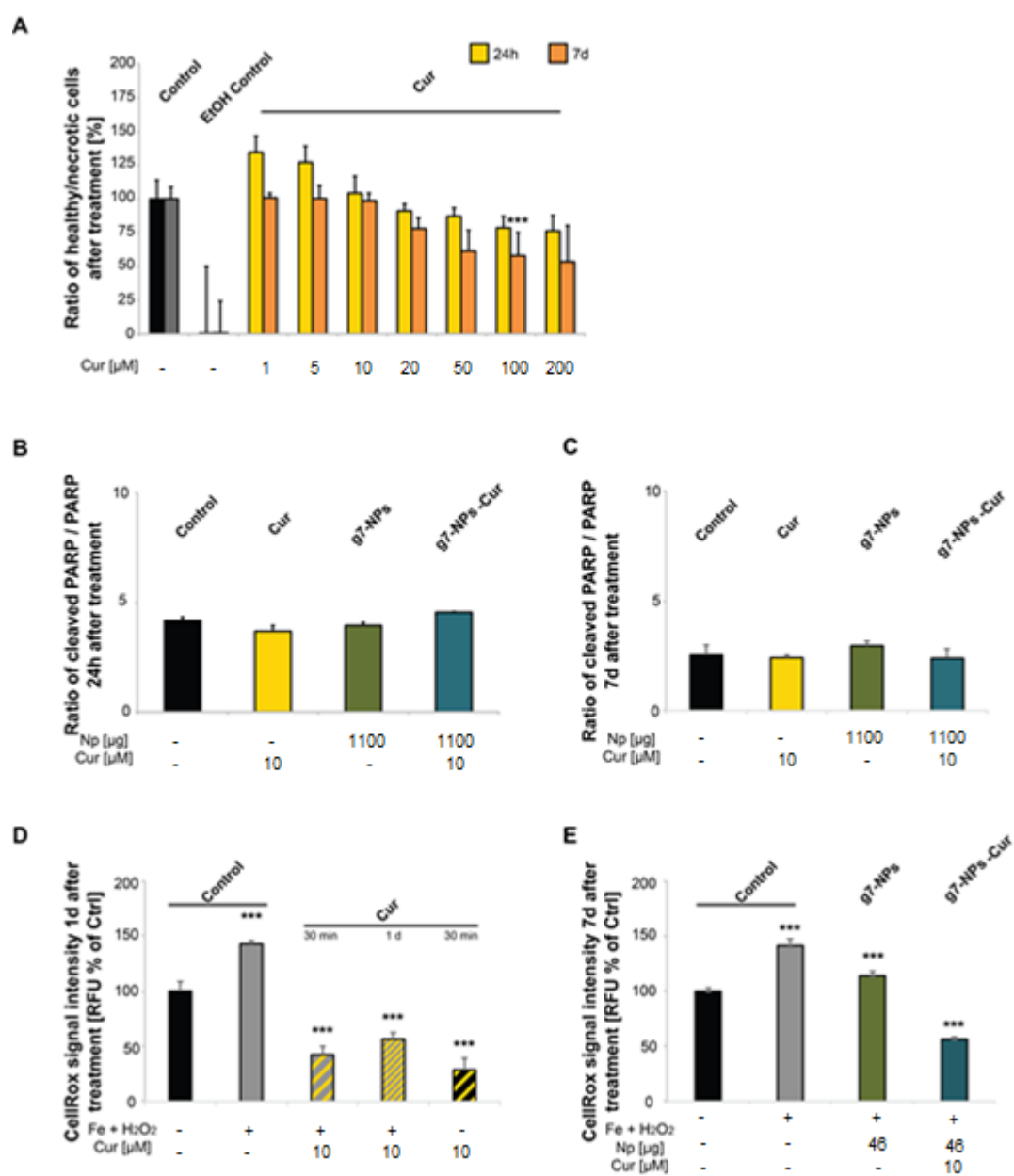
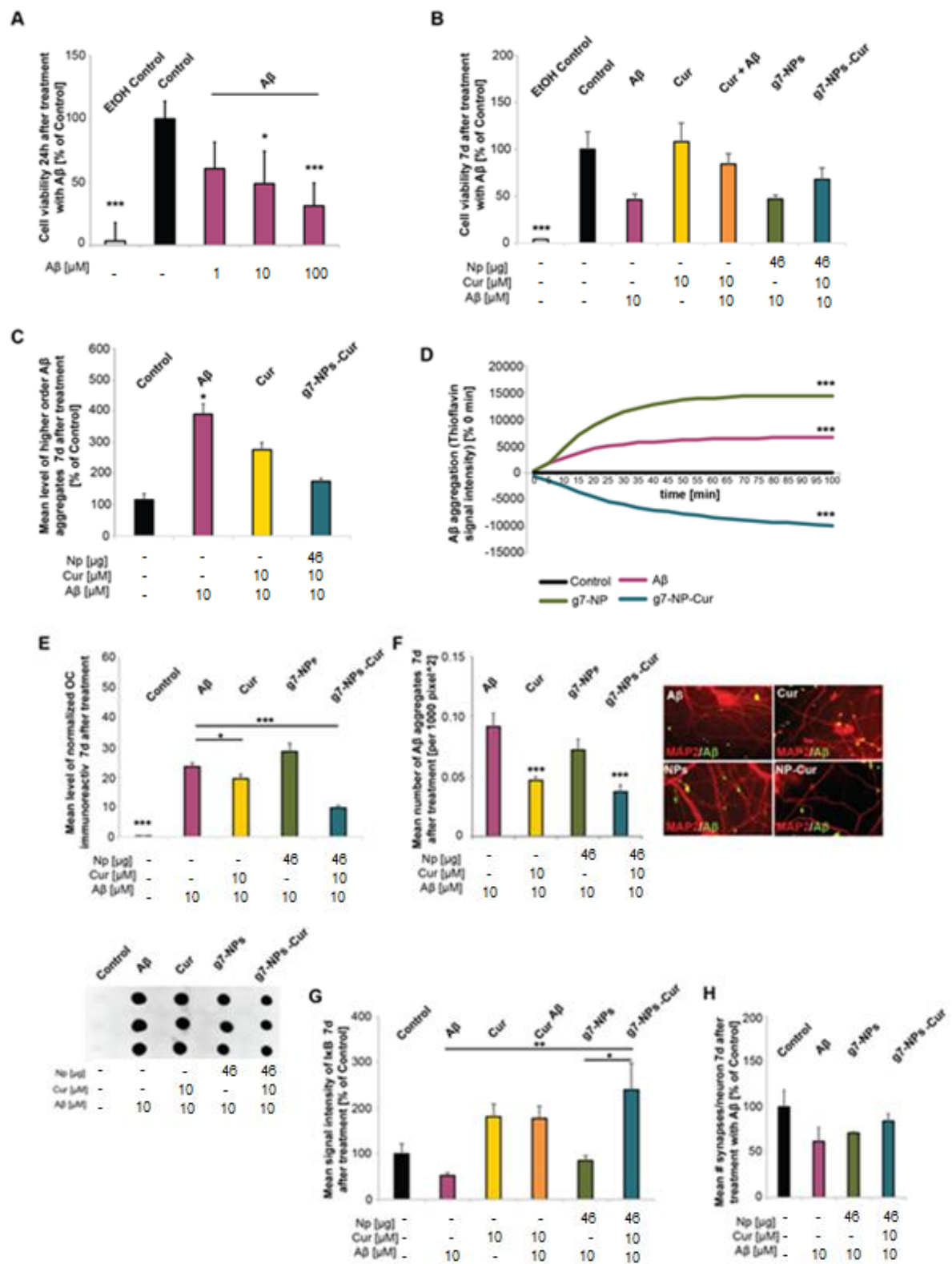


Figure 5



**Supplementary Material**

[Click here to download Supplementary Material: supplementary data\\_rev.docx](#)